Defence, Safety & Security
Oude Waalsdorperweg 63
2597 AK Den Haag
P.O. Box 96864
2509 JG The Hague
The Netherlands

www.tno.nl

T +31 88 866 10 00
F +31 70 328 09 61

TNO report

TNO 2022 R11422 | 2.0

Engineering Assessment of Effects on TACAN at Florennes and Simple Engineering Assessment Primary Surveillance Radar Beauvechain due to Wind Turbines Chastres-Walcourt

Date	6 September 2022
Author(s)	Onno van Gent Matijs Heiligers Stijn Dellevoet
Copy no	
No. of copies	
Number of pages	49 (incl. appendices)
Number of appendices	
Sponsor	Windvision, Belgium
Project name	Radar and Wind Turbine Interference Assessment
Project number	060.51414

Contents

1 Introduction

The performance of radar systems can be negatively influenced by wind turbines in their vicinity. EUROCONTROL has issued guidelines, on how to assess the potential impact of wind turbines [9]. Within these guidelines different zones around the radar are defined. A Detailed Engineering Assessment (DEA) for the primary radar is required at distances of the wind turbines ranging from 500 m to 15 km (zone 1). In the zone ranging from 15 km to the instrumented range of the primary radar (zone 2), a so-called Simple Engineering Assessment is required. For the secondary radars, a DEA needs to be performed in case the wind turbines are located closer than 16 km from the radar.

In this study the impact of wind turbines on performance of the primary radar at Beauvechain is assessed, following the EUROCONTROL guidelines for Primary Surveillance Radars (PSRs). Windvision has plans to build four wind turbines at Chastrès-Walcourt. The closest wind turbine is located at a distance of approximately 57 km from the radar, so outside 15 km from the radar. Therefore the Ministry of Defence requires a SEA to be performed for the PSR.

In addition to the PSR, the performance of a TACtical Air Navigation (TACAN) system, might be negatively influenced by wind turbines in the vicinity as well.

Windvision has requested TNO to perform an Engineering Assessment to investigate the influence of a new wind farm Chastrès-Walcourt on the Florennes Air Force Base TACAN system as well as to perform the SEA for the primary radar at Beauvechain.

In Chapter 2 the relevant input parameters of the wind turbines, the primary radar at Beauvechain and the TACAN system at Florennes are given.

Chapters 3 and 4 serve as a reference to the working principles of a TACAN system and the calculation of the radio wave reflections from wind turbines and the direct and indirect propagation paths that are relevant for this assessment.

The results of the assessment for the TACAN are shown as follows:

- Chapter 5: Line-of-sight analysis
- Chapter 6: DME range measurement errors
- Chapter 7: Bearing measurement errors

The result of the SEA of the PSR at Beauvechain are presented in Chapter 8, and finally in Chapter 9 the main conclusions are given.

2 Input Parameters

2.1 Wind turbines

The engineering assessment for the TACAN and the simple engineering assessment for the PSR at Beauvechain is carried out for the wind turbines shown in Figure 2.1. The yellow marked dots indicate the four wind turbines of the wind farm Chastrès-Walcourt under investigation. The cyan dots represent the locations of the 52 existing and authorised in a circle of 20 km around the newly planned wind turbines. The distance to the TACAN installation at Florennes measures approximately 14 km and to the primary radar at Beauvechain approximately 57 km.

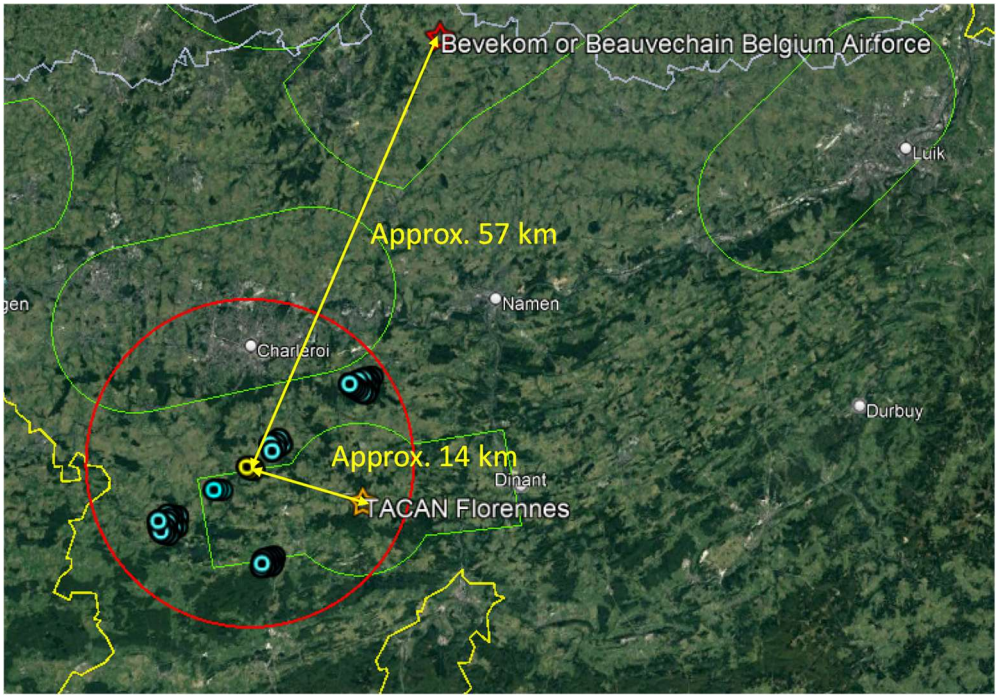

Figure 2.1 The locations of a newly planned wind farm Chastrès-Walcourt (yellow) as well as the locations of 52 existing and authorised wind turbines (cyan) in a circle (red) of 20 km around the newly planned wind turbines. Background image is taken from Google Earth.

In Table 2.1 an overview is presented of the positions, types, hub and tip heights of the 52 existing and authorised wind turbines within a distance of 20 km from the newly planned wind turbines. The positions, type of the wind turbines and tip height have been received from Windvision. The selected wind turbine type has been based on the defined rotor diameter, tip height and output power. The height of the ground level at the locations is given with respect to the EGM96 geoid and has been derived from the 1 arcsecond SRTM terrain height database.

Table 2.1 Overview of the positions, type and tip heights of the existing wind turbines within a 20 km distance from the newly planned wind turbines which have been provide by Windvision. The longitude, latitude have been derived from the Lambert72 coordinates and terrain heights are provided by Windvision. The longitude, latitude have been derived from these.

Nr.	Location	Lam72 X [m]	Lam72 Y [m]	Lat [°]	Long [°]	Terrain [m]	Type	Hub [m]	Tip [m]
1	Walcourt	160049	110940	50.30937	4.50982	229	MD77	85	123.5
2	Walcourt	158955	110308	50.30371	4.49444	239	MD77	85	123.5
3	Walcourt	159652	110455	50.30502	4.50423	241	MD77	85	123.5
4	Walcourt	159234	109503	50.29647	4.49834	231	MD77	85	123.5
5	Walcourt	159629	109850	50.29958	4.50389	237	MD77	85	123.5
6	Walcourt	160379	110335	50.30393	4.51443	238	MD77	85	123.5
7	Fosses-la-ville Mettet	170779	118567	50.37766	4.66088	242	E82	98	139
8	Fosses-la-ville Mettet	171282	118706	50.37889	4.66796	238	E82	98	139
9	Fosses-la-ville Mettet	168536	117843	50.37123	4.62931	232	E82	98	139
10	Fosses-la-ville Mettet	168857	117602	50.36905	4.63381	235	E82	98	139
11	Fosses-la-ville Mettet	169523	118202	50.37442	4.64320	234	E82	98	139
12	Fosses-la-ville Mettet	170145	118431	50.37646	4.65196	241	E82	98	139
13	Fosses-la-ville Mettet	170920	118223	50.37456	4.66284	248	E82	98	139
14	Fosses-la-ville Mettet	170454	118018	50.37274	4.65628	248	E82	98	139
15	Fosses-la-ville Mettet	169203	117372	50.36697	4.63866	240	E82	98	139
16	Fosses-la-ville Mettet	169629	117173	50.36517	4.64464	247	E82	98	139
17	Fosses-la-ville Mettet	170143	117307	50.36635	4.65187	253	E82	98	139
18	Fosses-la-ville Mettet	170795	117655	50.36946	4.66105	256	E82	98	139
19	Fosses-la-ville Mettet	170120	116856	50.36230	4.65152	259	E82	98	139
20	Fosses-la-ville Mettet	170797	117206	50.36542	4.66105	263	E82	98	139
21	Fosses-la-ville Mettet	170561	116740	50.36124	4.65771	263	E82	98	139
22	Cerfontaine	159751	96609	50.18053	4.50526	265	V90	78	123
23	Cerfontaine	159323	96473	50.17932	4.49926	258	V90	78	123
24	Cerfontaine	158873	96387	50.17855	4.49296	253	V90	78	123
25	Cerfontaine	158421	96243	50.17726	4.48663	247	V90	78	123
26	Cerfontaine	159594	95995	50.17502	4.50305	264	V90	78	123
27	Cerfontaine	159141	95939	50.17452	4.49670	265	V90	78	123
28	Cerfontaine	158696	95877	50.17397	4.49047	262	V90	78	123
29	Cerfontaine	158249	95814	50.17341	4.48421	261	V90	78	123
30	Cerfontaine	159449	95646	50.17188	4.50101	263	V90	78	123

Nr.	Location	Lam72 X [m]	Lam72 Y [m]	Lat [°]	Long [°]	Terrain [m]	Type	Hub [m]	Tip [m]
31	Cerfontaine	158616	95435	50.17000	4.48934	262	V90	78	123
32	Cerfontaine	158169	95384	50.16955	4.48308	264	V90	78	123
33	Beaumont (Froidchapelle)	145493	100738	50.21772	4.30559	235	GE 2.5 100	100	150
34	Beaumont (Froidchapelle)	145587	100205	50.21293	4.30691	247	GE 2.5 100	100	150
35	Beaumont (Froidchapelle)	145606	99830	50.20956	4.30718	256	GE 2.5 100	100	150
36	Beaumont (Froidchapelle)	145828	99475	50.20637	4.31029	256	GE 2.5 100	100	150
37	Beaumont (Froidchapelle)	146275	99935	50.21051	4.31655	250	GE 2.5 100	100	150
38	Beaumont (Froidchapelle)	146817	99123	50.20321	4.32415	252	GE 2.5 100	100	150
39	Beaumont (Froidchapelle)	146598	101490	50.22449	4.32106	227	GE 2.5 100	100	150
40	Beaumont (Froidchapelle)	147252	101341	50.22315	4.33023	229	GE 2.5 100	100	150
41	Beaumont (Froidchapelle)	147850	101278	50.22259	4.33861	236	GE 2.5 100	100	150
42	Beaumont (Froidchapelle)	146767	101004	50.22012	4.32343	233	GE 2.5 100	100	150
43	Beaumont (Froidchapelle)	147198	100842	50.21867	4.32948	243	GE 2.5 100	100	150
44	Beaumont (Froidchapelle)	146552	100605	50.21653	4.32043	240	GE 2.5 100	100	150
45	Beaumont (Froidchapelle)	147262	100356	50.21430	4.33038	244	GE 2.5 100	100	150
46	Beaumont (Froidchapelle)	147781	100053	50.21158	4.33765	254	GE 2.5 100	100	150
47	Beaumont (Froidchapelle)	147231	99874	50.20996	4.32994	248	GE 2.5 100	100	150
48	Beaumont (Froidchapelle)	146534	99573	50.20726	4.32018	256	GE 2.5 100	100	150
49	Beaumont (Froidchapelle)	146236	99252	50.20437	4.31601	256	GE 2.5 100	100	150
50	Fontenelle	152697	104680	50.253172	4.40656	233	V136*	112	180
51	Fontenelle	152203	104637	50.252788	4.39963	226	V136*	112	180
52	Fontenelle	153232	104633	50.252747	4.41406	220	V136*	112	180

* This windfarm has been granted for a 5 MW maximum wind turbine with a maximum rotor diameter of 140 m and a maximum tip height of 180 m. Final selection of a wind turbine has not yet been made. Therefore a V136 with a output power of 4.5 MW, a hub height of 112 m and a rotor diameter of 136 m has been taken as a representative type.

The positions and dimensions of the newly planned wind turbines (New-WT1 to New-WT4) are presented in Table 2.2. The information has been provided by Windvision. The wind turbines will have a maximum tip height of 180 m above ground level (AGL).

Table 2.2 Overview of the positions of the four newly planned wind turbines. The X, Y coordinates have been provided by Windvision. The longitude and latitude have been derived from the Lambert72 coordinates. The terrain height, reference to EGM96, has been derived from the SRTM1 altitude database.

Nr.	ID	Lambert72 Coordinates		Terrain height	Lat. WGS84	Lon. WGS84	Tip Height AGL
		X [m]	Y [m]	Z [m]	[º]	[º]	[m]
53	New WT1	156179	107514	203	50.27863	4.45543	180
54	New WT2	156754	107520	210	50.27867	4.46350	180
55	New WT3	156535	107226	204	50.27603	4.46042	180
56	New WT4	157116	107215	205	50.27593	4.46857	180

No final selection of the wind turbine type have been performed yet. There are three potential candidates to select from. The N131 Delta from Nordex, the V126 from Vestas both with a tip height of 180 m, and the GE-3.8-130 from General Electric with a tip height of 175 m. The main dimensions of these three candidates are listed in Table 2.3.

Table 2.3 Three potential wind turbine candidates and the derived worst-case and their dimensions

Manufacturer	Model	Output Power [MW]	Hub height [m]	Rotor diameter [m]	Tip height [m]
Nordex	N131 Delta	3.6	114	131	180
Vestas	V126	3.45	117	126	180
GE	GE-3.8-130 LNTEs	3.8	110	130	175

This worst-case approach with a maximum hub height of 117 m and maximum rotor diameter of 131 m results in a theoretical tip height of 182.5 m AGL. However when the final selection is performed, the final tip height will never exceed 180 m AGL, according to Windvision. This worst-case approach also covers other representative wind turbines within the same power range and maximum tip height.

Note: After finishing the assessment study it became clear that the wind turbines at Fontenelle will not be build. As can been observed in Chapter 5 for the TACAN and Chapter 8 for the SEA, the effects of these wind turbines do not overlap with the effects that the newly planned wind turbines may cause.
In addition to this, two more wind turbines at Walcourt Florennes Gerpinnes have be granted. These two will have the Lambert '72 coordinates X:160731 Y:110787 and X:161100 Y:111231 and are situated north east from the current wind farms at Walcourt, so at an even larger distance from the newly planned wind turbines than the current wind turbines at Walcourt.

2.2 TACAN System Florennes

The analysis is done for the TACAN navigation system at Florennes AFB. The system parameters that are relevant for this study are presented in Table 2.4. This information has been taken from the eAIP of Belgium and Luxembourg [1]. According to the eAIP the TACAN uses channel 52X, which implies transmission at 1013 MHz while it receives interrogation signals at 1076 MHz.

Table 2.4 Relevant system parameters of the TACAN Florennes taken from eAIP Belgium and Luxembourg [1].

Parameter	Value
ID	BFS
Frequency	CH 52X
Latitude (WGS84)	50°14'29.1" N
Longitude (WGS84)	4°39'11.7" E
Elevation	952 ft

In Lambert'72 coordinates the location of the TACAN is converted as shown in Table 2.5.

Table 2.5. TACAN location converted from WGS84 to Lambert'72 coordinates.

Parameter	Value
Lambert'72 X [m]	170295
Lambert'72 Y [m]	103409
Height EGM96 Z [m]	290

Figure 2.2 shows the location of the TACAN at the Florennes AFB as well as a zoomed image.

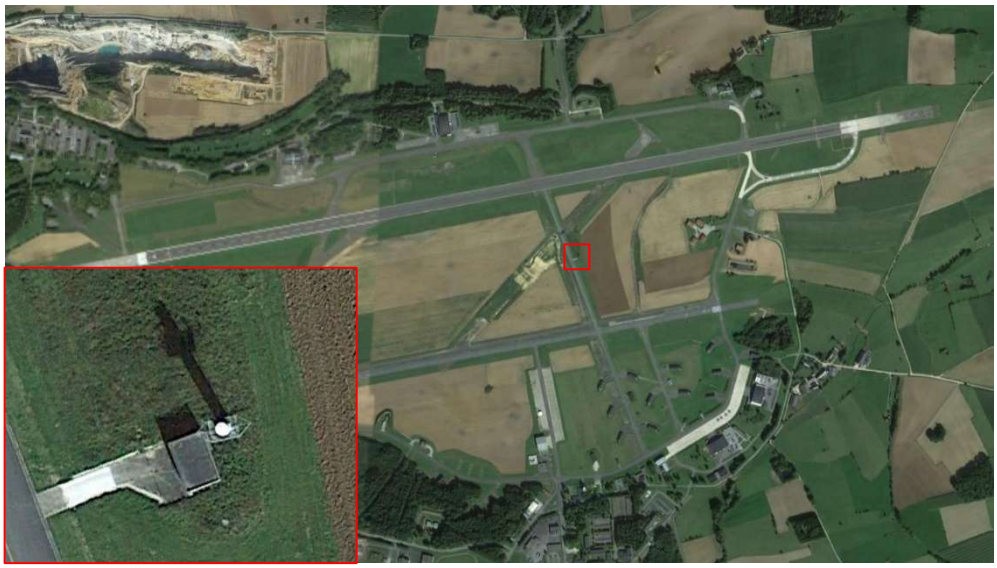

Figure 2.2. Location of the Florennes TACAN. Imagery is taken from Google Earth.

2.3 Primary Radar System Beauvechain

The Beauvechain air base (Figure 2.3) is equipped with a combined radar system and consists of both a Primary Surveillance Radar (PSR), the Thomson CSF TA-10M and a Secondary Surveillance Radar (SSR). The PSR has been upgraded by Intersoft-Electronics at a later stage.

Figure 2.3 The Airport Surveillance Radar at Beauvechain Air Base (image: Google Earth).

In this study only the PSR is under investigation. The radar parameters that are relevant for this study are presented in Table 2.6. This information has been taken from the radar file ASR Beauvechain [10] provided by the Belgium Ministry of Defence and updates received via email [11].

Table 2.6 Relevant radar parameters of the PSR Beauvechain taken from [4] and [5].

Parameter	Value
Antenna position	
X (Lambert 72)	178660
y (Lambert 72)	160163
Latitude (WGS84)	50° 45’ 04.58’’ (50.751273) N
Longitude (WGS84)	4° 46’ 29.58’’ (4.774882) E
Height (EGM96)	13m AGL
	135 m AMSL
Antenna rotation speed	12 rpm
Instrumented range	100 NM (185 km)
Horizontal beamwidth (-3 dB)	1.5 ± 0.2°
Range cell	
Depth	21.9 m
Width	0.147°
CFAR	
Type	CAGO (Cell Averaging Greatest of)
Number of range cells within the early and late window	24 (Per window)
Number of guard cells on each sides of the CUT	12

2.4 Terrain data model

For consistency reasons the terrain elevation data as used in TNO’s simulation environment is based on the validated US Shuttle Radar Topography Mission[1]

[1] For the line-of-sight analysis the data from the Shuttle Radar Topography Mission (SRTM1) is used. This database contains terrain altitude information with respect to the EGM96 geoid. The database was determined by NASA using high-resolution radar carried on the Space Shuttle. The

(SRTM1) with 1 arc-second resolution. The elevations might deviate from a locally published terrain elevation map.

SRTM1 data has a resolution of 1 arcseconds, which corresponds to a horizontal resolution of about ~20 m at 51 degrees latitude.

3 TACAN operation

This chapter provides an easy to read explanation of TACAN. It is largely an amalgamation of [2], [3], and [4].

TACAN stands for Tactical Air Navigation System and is a navigation system for military use. The TACAN is a military radio navigation aid to determine aircraft relative range and bearing. Bearing and distance signals require only a single transceiver on the ground and on the aircraft. They also use the same UHF frequency.

The TACAN shape is (has been for a long time) a vertical cylinder, see Figure 3.1a.

a. A US Air Force TACAN antenna, from [4]

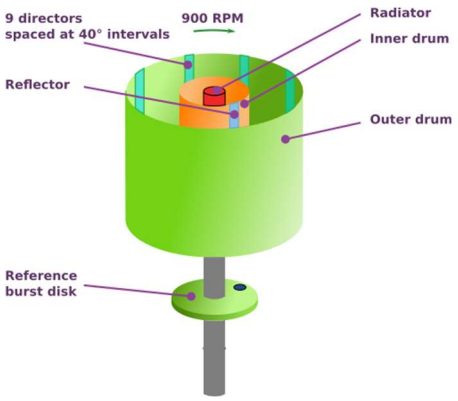

b. Rotating parasitic elements in TACAN antenna, from Reference [2].

Figure 3.1 The TACAN antenna.

A rotating drum with a reflector electrically adjusts the radiation pattern, adding a signal dip (low gain) that rotates at 900 RPM, which is equivalent to a 15 Hz amplitude modulation. The radiation pattern in the horizontal plane takes the shape of a cardioid, as is shown in Figure 3.2a. Another drum with a set of 9 directors, mechanically linked to the first one, creates a 135 Hz (9x15) additional amplitude ripple over the 15 Hz modulation, as is shown in Figure 3.2b.

The TACAN does not transmit a signal continuously, but the signal is keyed (transmitter switched on/off) by bursts of information. There are five different burst types:

- Main Reference Burst (MRB)
- Auxiliary Reference Burst (ARB)
- Responses to DME interrogations
- Burst for identification of the TACAN
- Squitter bursts

For TACAN systems with X channels all burst types contain one or more pulse pairs with a pulse repetition interval of 12 µs as shown in Figure 3.3.

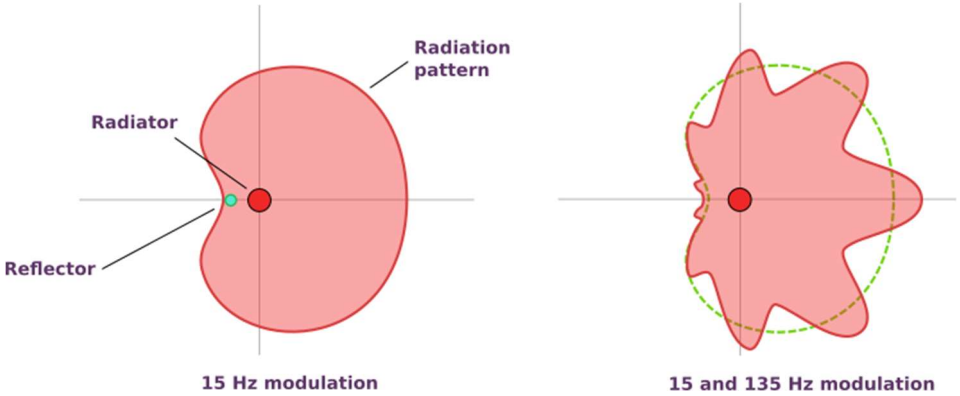

a. A US Air Force TACAN antenna, from [2].

b. Rotating parasitic elements in TACAN antenna, from [2].

Figure 3.2 TACAN 15 Hz and 135 amplitude modulation patterns.

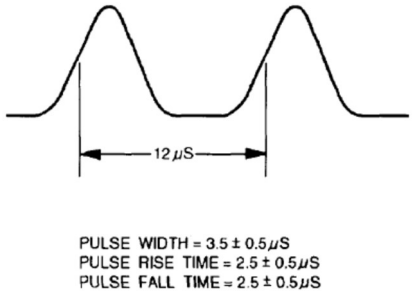

Figure 3.3 TACAN interrogation pulse pair, from [5].

3.1 Main Reference Burst

While the antenna drums rotate, the ground station transmits a Main Reference Burst (MRB) that informs receivers that the antenna faces the reference direction, usually the magnetic north. For an X channel TACAN the MRB contains 12 pulse pairs with 12 μs spacing between the pairs. This burst is transmitted at a rate of 15 Hz (i.e. at every antenna rotation).

By comparison of the phase of the 15 Hz modulated signal during reception of the MRB, the aircraft is able to determine its own bearing relative to the station. For example if the receiver senses that the received signal is weakest during reception of the MRB, it knows that it is located south of the TACAN.

3.2 Auxiliary Reference Burst

To be able to refine the bearing estimation, the TACAN also transmits Auxiliary Reference Bursts (ARB) at a rate of 135 Hz at the magnetic directions 040°, 080°, 120°, 160°, 200°, 240°, 280°, and 320°. For an X channel TACAN the ARB contains 6 pulse pairs with 24 μs spacing between the pairs. Therefore the ARB can be distinguished from the MRB.

By comparison of the phase of the 135 Hz modulated signal during reception of the ARB, the aircraft is able to determine its own bearing relative to the station within a 40° sector as is already known from the bearing estimation on the 15 Hz signal.

Figure 3.4 shows the 15 Hz and 135 Hz modulations and the phase of these modulations during the reception of the reference bursts.

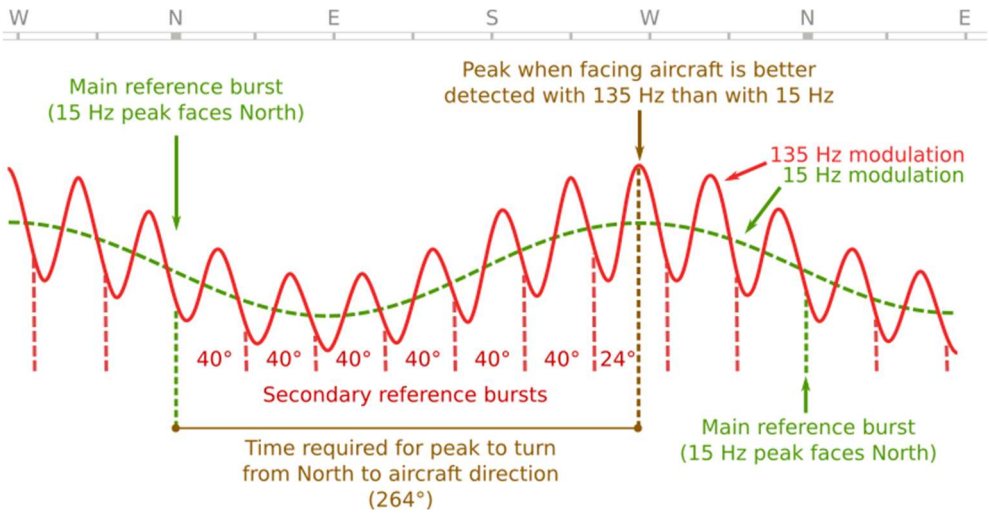

Figure 3.4 Transmitted signal, with reference signals, in a given direction. From [2].

3.3 Responses to DME interrogations

Distance is measured by determining the time delay between an interrogation transmission and the received response. The aircraft transmits an interrogation signal (pulse pair). In response, the TACAN retransmits this signal with a predefined delay of 50 µs (see Figure 3.5). This is described in more detail in [5].

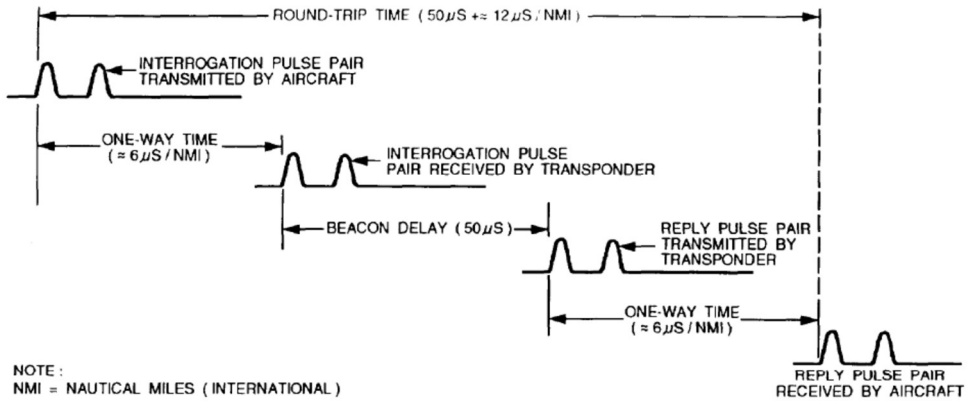

Figure 3.5 Distance measuring round trip travel time, from [5]

In order not to reply to interrogations as received by multipath, a dead time after reception of the first pulse pair is implemented during which the TACAN does not react to any interrogations.

3.4 Identification bursts

Before bearing and distance information can be used, first an aircraft has to identify the TACAN. Only after positive identification the aircraft knows that the signals of the correct TACAN is received. The identification is based on Morse code of the 3

letter designator of the TACAN. About every 30 seconds all distance and bearing transmissions are stopped to send the identification burst.

The duration of a Morse dot is 100 to 125 ms, and for a dash 300 to 370 ms. During transmission of a Morse dot or dash, repeatedly two 12 µs-pulse pairs with 100 µs spacing are transmitted with a rate of 1350 Hz. It can be observed that the total length of an identification burst can take about 2 to 4 seconds. After completion of the burst, the TACAN again starts transmitting the reference bursts and interrogation replies.

3.5 Squitter bursts

In order for the aircraft to receive sufficient pulses to determine the phase of the amplitude modulated signal, the TACAN system is designed to transmit 2700 to 3600 pulse pairs per seconds, i.e. 300 to 400 pulse pairs per antenna rotation. In the case that there are only few interrogation requests, the number of transmitted replies is supplemented by randomly spaced squitter bursts.

4 Wind turbine RCS and multipath

The wind turbine consist of three parts, each having their own contribution to the overall wind turbine RCS:

- The wind turbine blades
- The pole
- The nacelle

Moreover, for TACAN one is interested in the so called bistatic RCS, this is the radar cross section the object has if the direction of the incident wave does not coincide with the direction of the reflected wave. (Note: with radar, one needs the monostatic RCS, the reflection back to the radar, hence incident wave direction = reflected wave direction).

Where in this document the acronym RCS is used, the bistatic RCS is meant. The monostatic RCS will be explicitly mentioned, if applicable.

The radar cross section σ_w models used for pole, nacelle, and blade are the ones also applied in the TNO model PERSEUS.

4.1 Blade RCS

The RCS differs strongly in accordance to the angles of incident and reflected wave, as depicted in a general way for a section of the blade in Figure 4.1.

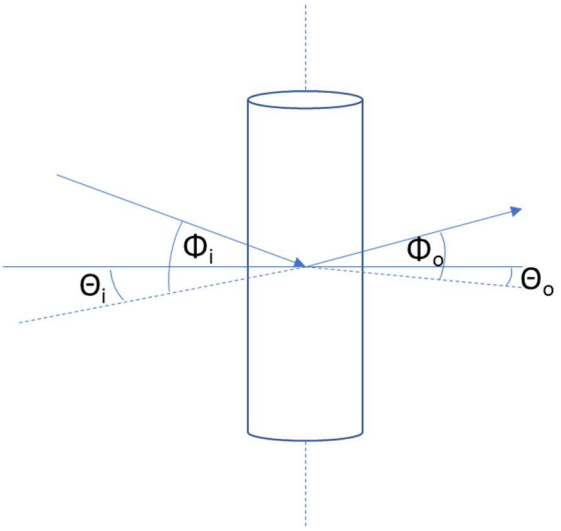

Figure 4.1 Blade with incident and reflected wave direction.

The blades rotate and moreover the nacelle is turned towards the wind. As a result, the blades can have any position, including that providing maximum RCS. In this document this maximum RCS is taken into account. One should note however that, due to the rotation of the blade, this condition is only valid for a short time.

In the condition of a stationary rotor, the optimum would only occur for a specific direction. The aircraft can be in this direction, however only for a short moment, due to the movement of the aircraft.

The bistatic RCS of the blade is modelled as an elongated ellipsoid with defined blade length *a*, width *b*, and thickness *c*. The bistatic RCS can be calculated as:

$$\sigma = \pi \frac{a^2 b^2}{c^2} \frac{4}{(1+\cos\beta) + \frac{b^2}{c^2}(1 - \cos\beta)}$$

The angle *β* is the angle between the line of incidence and the line of reflection.

4.2 Pole RCS

The RCS of the pole is modest, except if the incident angle equals the reflection angle. For cylindrical poles, with the TACAN transmitter close to the horizon, incident and reflected wave are both perpendicular to the pole, so the high RCS is only discerned at very low elevation angles.

For cone-shaped poles, the reflection is discernible at low angles, see Figure 4.2. Note that the angles are exaggerated. A typical value for β is 2°. The horizontally travelling TACAN signal is reflected in a cone of β from horizontal.

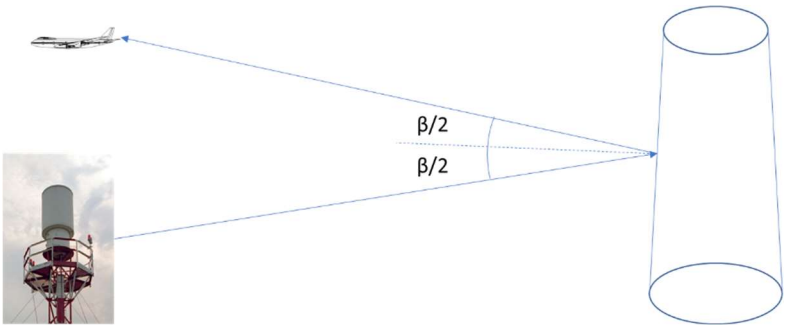

Figure 4.2 Pole RCS

Note that due to the Earth's curvature, only a part of the cone is illuminated by the TACAN system.

Since for the vast majority of possible aircraft locations the pole RCS is small compared to the maximum attainable RCS of the wind turbine's blade, the pole RCS is not taken into account separately.

4.3 Nacelle RCS

The RCS of the nacelle is small compared to the RCS of blade and pole and is neglected in the study.

4.4 Multipath

The pulses that are transmitted by either the TACAN or the aircraft, travel via a direct path to the aircraft or TACAN respectively. The presence of a wind turbine also causes an indirect path by reflecting part of the pulse. This phenomenon is called multipath. The relative geometry of TACAN, aircraft and wind turbine is

shown in Figure 4.3. In this graph, ϕ is the angle between the line TACAN-aircraft and TACAN-wind turbine. Θ is the elevation angle of the aircraft as seen from the TACAN.

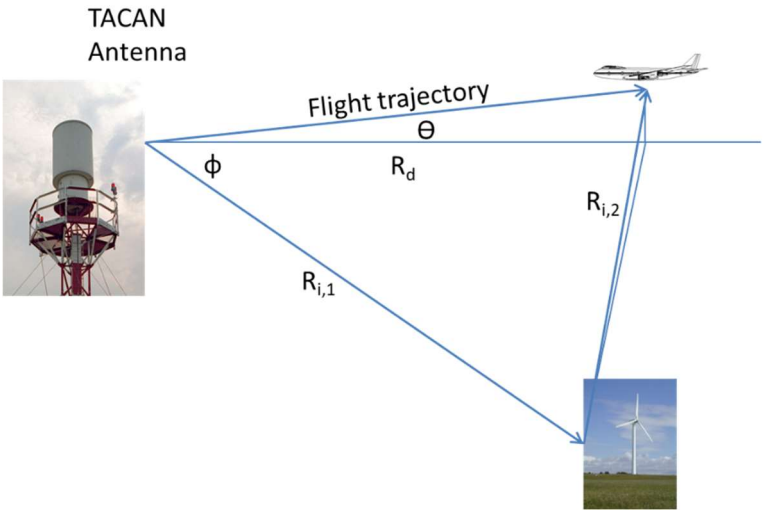

Figure 4.3 Geometry of TACAN, aircraft and wind turbine.

For the power of the direct path (P_d) without reflection at the wind turbine, the radio equation yields:

$$P_d = \frac{P\ G_t}{4\pi\ R_d^2} \cdot \frac{A_{eff}}{L_d} = \frac{P\ G_t\ G_r\ \lambda^2}{(4\pi)^2\ R_d^2\ L_d}$$

P is transmit power, G_t is transmit antenna gain, A_{eff} is the area of the effective antenna aperture (on receive), R_d is the length of the direct path, L_d represents losses along that path, λ is wavelength, G_r is the receive gain.

The indirect power, which includes the reflection at the wind turbine, is given by:

$$P_i = \frac{PG_t}{4\pi R_{i,1}^2} \cdot \frac{\sigma_w}{4\pi R_{i,2}^2} \cdot \frac{A_{eff}}{L_i} = \frac{PG_tG_r\lambda^2\sigma_w}{(4\pi)^3 R_{i,1}^2 R_{i,2}^2 L_i}$$

in which σ_w denotes the bistatic radar cross section (RCS) and L_i denotes losses along the indirect path. Assuming losses are equal along both paths, the power ratio is given by:

$$\frac{P_i}{P_d} = \frac{\sigma_w R_d^2}{4\pi R_{i,1}^2 R_{i,2}^2}$$

The radar cross section σ_w of the wind turbine is modelled in the same way as it is modelled in PERSEUS. The power ratio is used in the next chapter to determine the distance and bearing accuracy.

5 TACAN Line of Sight Analysis

Using the input parameter information of Chapter 2, a line-of-sight analysis has been carried out. In Figure 3.1 the terrain profile is shown in the area containing the wind turbines and TACAN. The terrain profile has been obtained from the SRTM1 database. The lines in the figure connect the TACAN to the planned wind turbines. By studying the terrain profile along this line, it can be determined whether the TACAN will have line-of-sight to the windfarm.

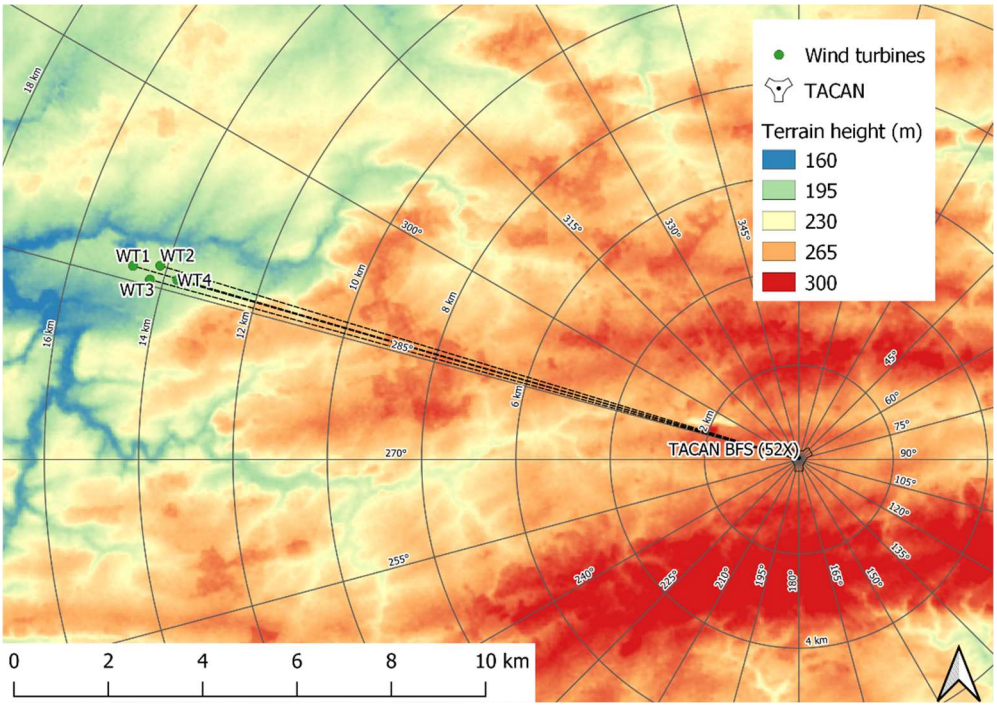

Figure 5.1 The altitude of the terrain between TACAN and wind turbines taken from the SRTM1 database. The altitude in this image varies from +150 m (blue) to +350 m (red) AMSL. The line-of-sight analysis is performed by studying the terrain profile on the line connecting the TACAN and each wind turbine.

So-called ‘standard propagation’ is assumed when determining the line-of-sight. This is modelled by multiplying the earth radius by a factor of 4/3 (the “k-factor”).

Figure 5.2 shows line-of-sight diagrams between the location of the TACAN and the newly planned wind turbine locations. The x-axis shows range over ground in kilometres calculated using Vincenty’s formulae. The turbines are located between approximately 13.7 and 14.7 km from the TACAN.

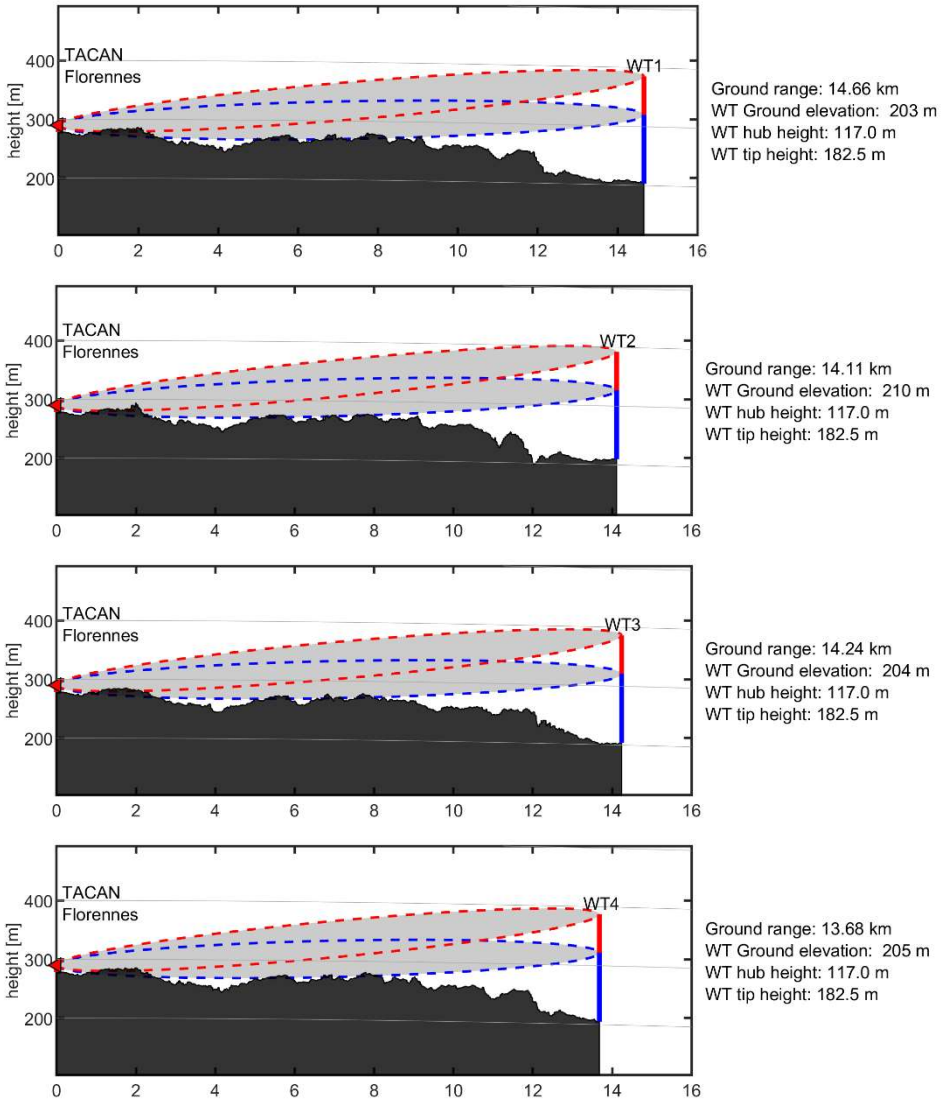

Figure 5.2 Line-of-sight between the TACAN and wind turbines with first Fresnel zones between the TACAN and the wind turbine's hub (blue) and tip (red).

For the wind turbines WT1 to WT4 the (red) Fresnel zones between the TACAN and the highest tip of the blade are not significantly obstructed by the terrain profile. This means that the TACAN has line-of-sight to the blades of the wind turbines when they are in the top half of their rotation. The paths between TACAN and all wind turbines' masts are largely obstructed by the terrain and therefore the masts are not in the line-of-sight of the TACAN.

6 DME distance accuracy

To determine the DME distance measurement accuracy, it is assumed that a blade is in a position providing maximum reflection towards the aircraft (worst case assumption).

6.1 Propagation

DME is based on the travelling of radio waves in both directions between an aircraft (interrogator) and TACAN (transponder). The DME analysis is done for the propagation channel, from TACAN antenna to aircraft antenna. This channel is reciprocal, which means the channel has the same characteristics, irrespective of the signal direction. It is assumed that TACAN behaviour is equal for both directions.

6.2 Error mechanism

In order for a reflected pulse pair to elicit a second TACAN response, two conditions have to be met that are explained more in detail in the sections that follow:

- The delay between the two pulse pairs needs to be more than the “dead time”;
- The signal strength shall be above the TACAN receiver threshold.

6.2.1 Dead time

As can be seen from Figure 4.3, there will be a difference in path length between the direct and indirect path:

$$\Delta R = (R_{i,1} + R_{i,2}) - R_d$$

The TACAN receiver needs to be able to separate the direct interrogation pulse pair from the indirect/reflected interrogation pulse pair. In theory, given that the pulses in a pulse pair are 12 µs apart (see Figure 3.3), the second interrogation pulse pair needs to be delayed by about 24 µs in order to be detected as a separate pulse pair.

The dead time, the time the TACAN system does not respond to a second interrogation, is much larger than 24 µs. The dead time is a mechanism that is used to prevent the TACAN system to react to multipath. The specification [8] states “The dead time shall not normally exceed 60 µsec”, a minimum value however is not specified. Literature [6] indicates the dead time is “about 60 µsec”. In this report, the dead time is considered to be relatively short, 50 µs, which is a worst case assumption. This implies that, to trigger a second TACAN response, the difference in path length would be at least:

$$\Delta R = 50\ \mu s \times c = 15\ \mathrm{km}$$

Where *c* is the speed of light (300.000 km/s).

In case the interrogation pulse pair is delayed by more than 50 µs, it can trigger the TACAN transponder to transmit a second response to the same, but delayed

interrogation request. If the delay is less, triggering will not occur due to the dead time of the transponder.

6.2.2 *Sensitivity*

TACAN sensitivity is not specified in [8]. In [5] it is indicated that the maximum measuring distance can be as large as 200 Nautical Mile or 370 km. Assuming a margin of 6 dB in receiver sensitivity, responses can be triggered up to 740 km under favourable conditions. Other literature [6] is more exact and claims -92 dBm receiver sensitivity.

In this report a receiver threshold is assumed which allows the TACAN system at a distance of 370 km reliably being received with 6 dB margin.

6.3 DME error results for the wind turbines

For the wind turbines, the relative signal strength of the indirect interrogation pulse pair (reflected at the wind turbine) has been calculated. For the subsequent wind turbines, the results are shown for aircraft at an altitude *H* of 305 m AGL (1000 ft) and for ϕ = 0°, ϕ = 8°, ϕ = 16°, and ϕ = 24° respectively. This geometry is shown in Figure 6.1.

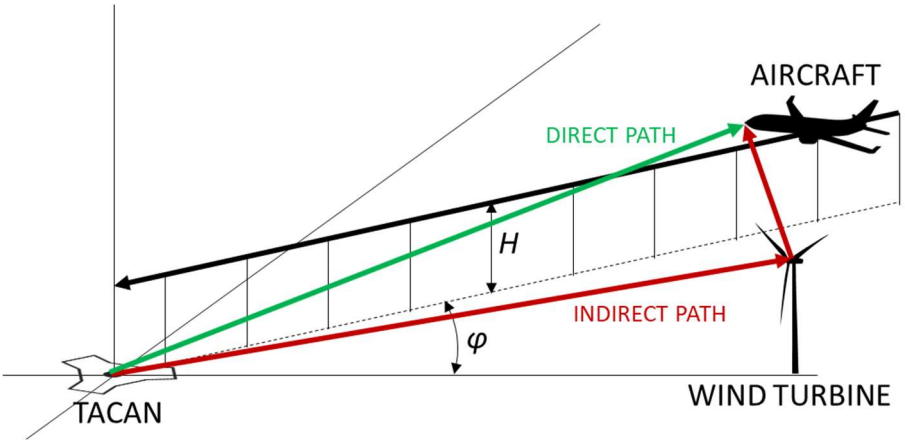

Figure 6.1 DME error geometry as used in the analysis.

As explained in Section 6.2, a DME “error” indicates that both:

- The path length difference of the direct and the indirect paths is more than 15 km (or 50 µs delay)
- The relative signal strength is large enough to evoke a response of the TACAN system.

In the figures these two conditions are depicted by the dashed red and blue curves. The red curve is related to the path length difference. The blue curve is related to the relative signal strength. Only when for a certain ground range between TACAN and aircraft (horizontal axis) both solid curves are above their dashed counterparts, a DME range error is possible. If this condition exists, it is indicated by a yellow bar in the graph. Absence of the yellow bar means no DME error.

In case that the two error conditions are met, the path length difference is the DME distance error that might appear on the navigation display in the airplane. This situation only occurs for the most unfavourable position of the wind turbine blade

(worst case scenario). The probability of the blade being in this position is very low (in the order of 10^{-4}). Moreover, the wind turbine is rotating and the aircraft is moving, so this most unfavourable position lasts only for a second at most. Even in the unlikely event an erroneous response of the TACAN is evoked, this will only happen once. It should be noted that, should a TACAN death time of 60 µs be used, the probability of erroneous TACAN DME responses would be close to zero.

In addition, the receiver in the aircraft is equipped with an “echo cancellation”. The second TACAN DME response (which arrives with 50 µs delay or more) is neglected by the aircraft.

6.3.1 DME errors for WT1

The graphs show no DME errors for all trajectories. For higher altitudes the DME errors are smaller compared to the lower altitudes. Therefore only the results that correspond to an aircraft altitude of 305 m AGL are shown.

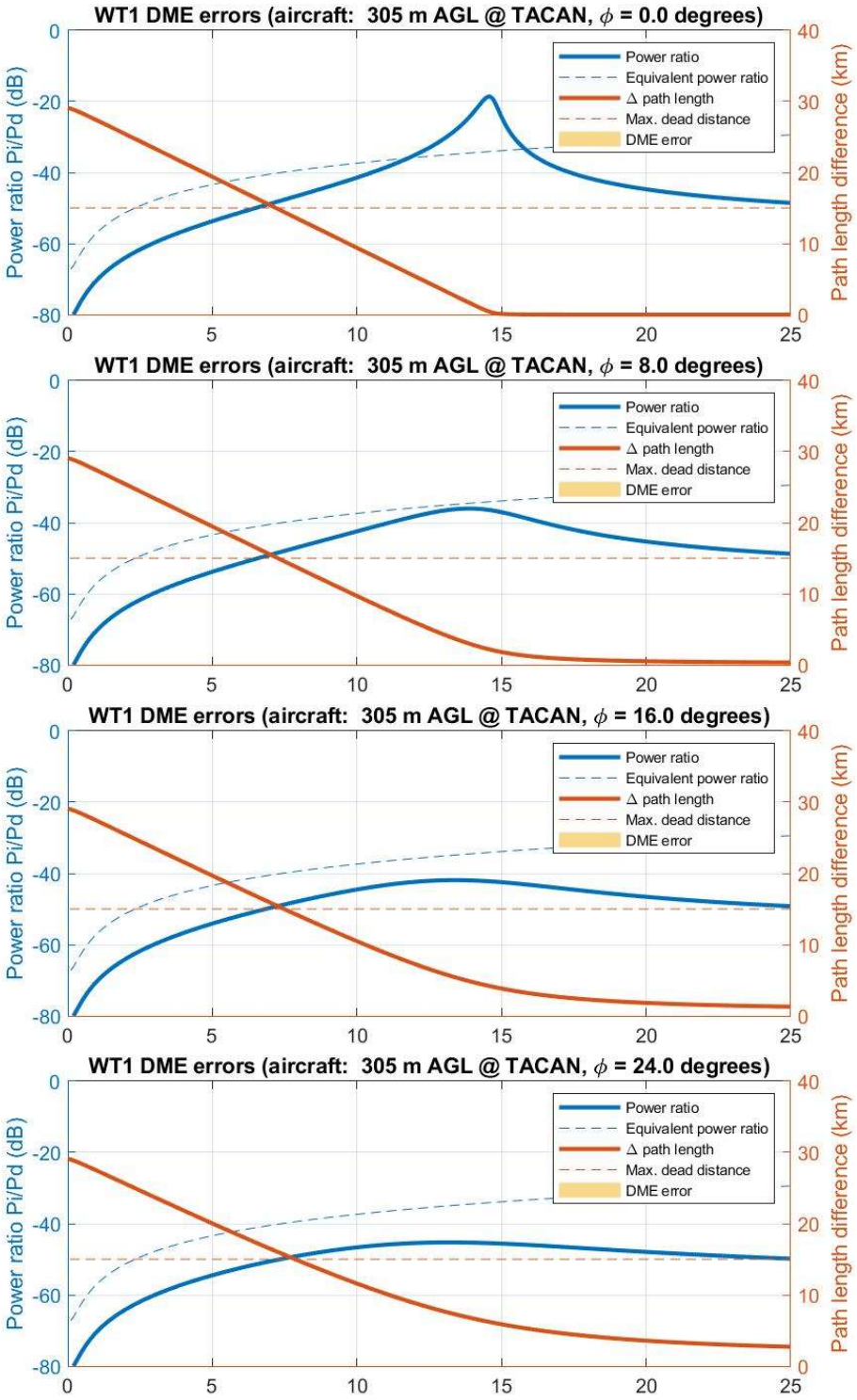

Figure 6.2 Relative signal strength and path length difference along flight trajectory. Flight trajectory altitude is 305 m AGL and angle ϕ = 0°, ϕ = 8°, ϕ = 16°, and ϕ = 24°

6.3.2 DME errors for WT2

The graphs show no DME errors for all trajectories. For higher altitudes the DME errors are smaller compared to the lower altitudes. Therefore only the results that correspond to an aircraft altitude of 305 m AGL are shown.

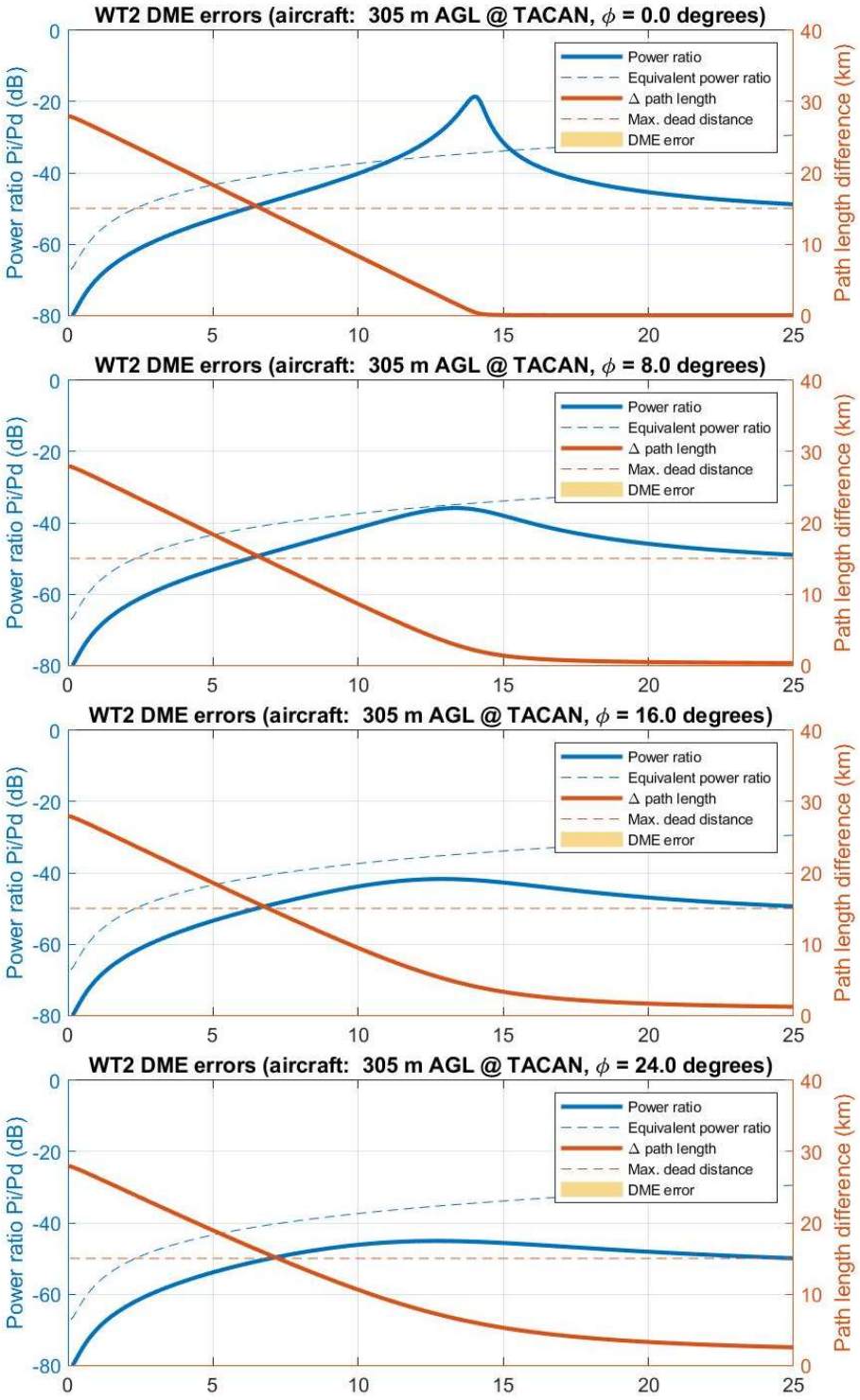

Figure 6.3 Relative signal strength and path length difference along flight trajectory.
Flight trajectory altitude is 305 m AGL and angle ϕ = 0°, ϕ = 8°, ϕ = 16°, and ϕ = 24°

6.3.3 DME errors for WT3

The graphs show no DME errors for all trajectories. For higher altitudes the DME errors are smaller compared to the lower altitudes. Therefore only the results that correspond to an aircraft altitude of 305 m AGL are shown.

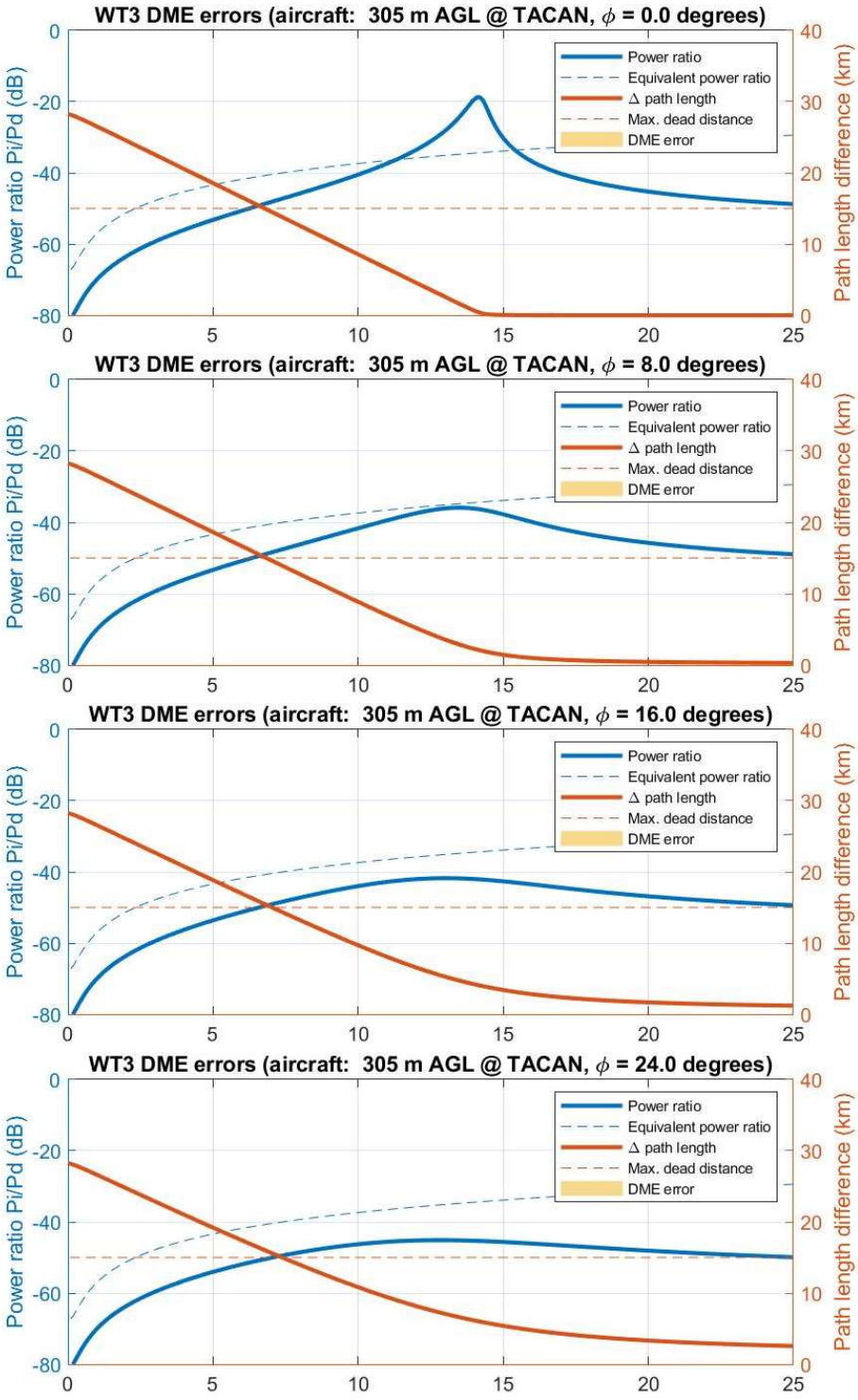

Figure 6.4 Relative signal strength and path length difference along flight trajectory.
Flight trajectory altitude is 305 m AGL and angle ϕ = 0°, ϕ = 8°, ϕ = 16°, and ϕ = 24°

6.3.4 DME errors for WT4

The graphs show no DME errors for all trajectories. For higher altitudes the DME errors are smaller compared to the lower altitudes. Therefore only the results that correspond to an aircraft altitude of 305 m AGL are shown.

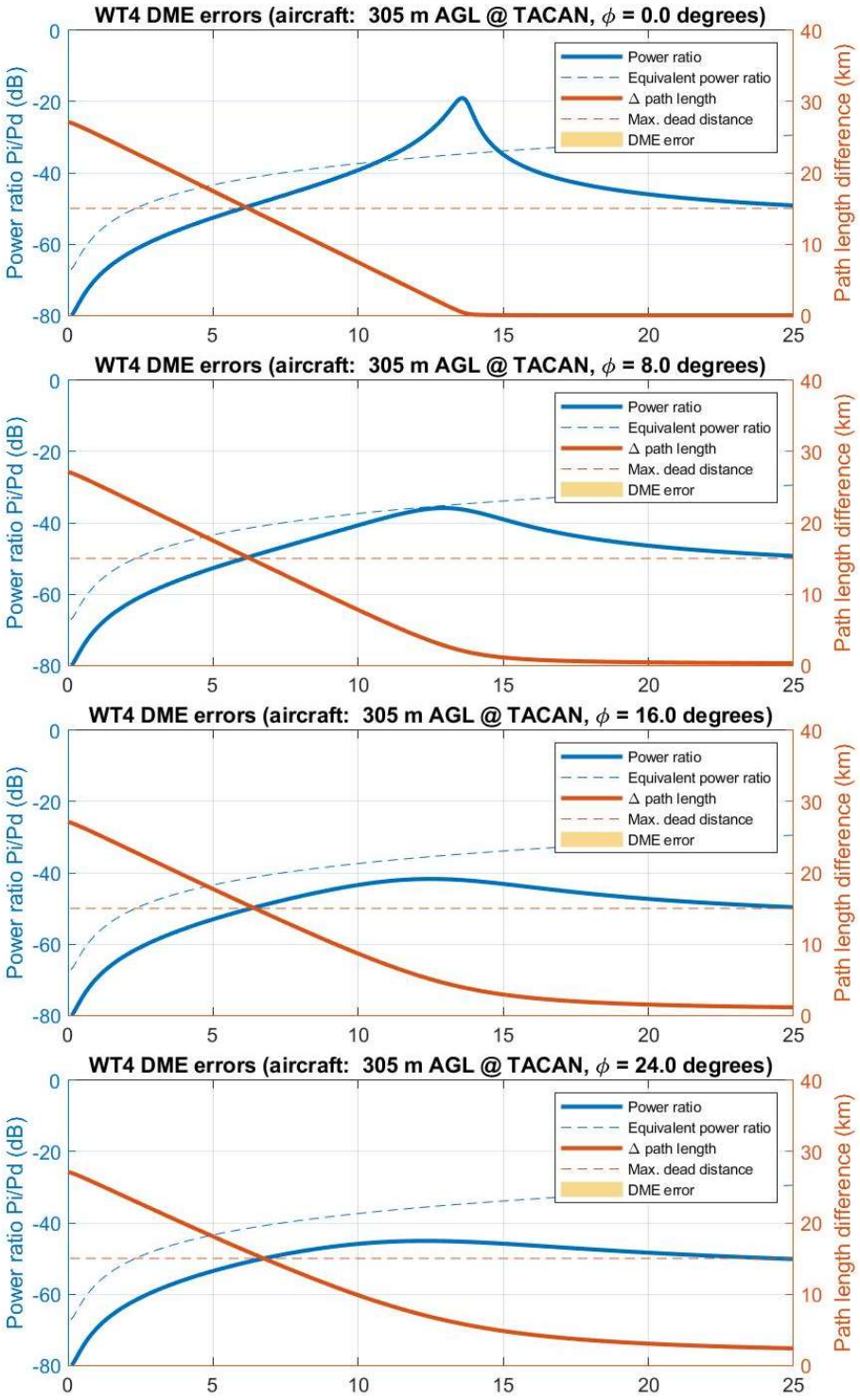

Figure 6.5 Relative signal strength and path length difference along flight trajectory.
Flight trajectory altitude is 305 m AGL and angle ϕ = 0°, ϕ = 8°, ϕ = 16°, and ϕ = 24°

6.4 Consequences for TACAN DME accuracy

The assessed wind turbines WT1 – WT4 will not evoke erroneous TACAN DME transmissions even in the most unfavourable position of the wind turbine blade.

Under nominal conditions, possible performance degradation of the TACAN system will be much less than considered here.

7 Bearing accuracy

The aircraft relies on these signals that are transmitted by the TACAN system (see Figure 3.4):

- The main and auxiliary reference bursts
- The 15 Hz and 135 Hz amplitude modulated pulse pair signals

The bearing to the TACAN is determined by measuring the phase relation between the reference bursts and the amplitude modulation of the 15 and 135 Hz signals.

7.1 Error mechanisms

There are two mechanisms that potentially cause errors to the bearing measurements:

- Delay (time-shift) of the detected peaks of the reference bursts due to multipath.
- Phase shift of the measured AM-modulation due to multipath

7.1.1 Delay (time-shift) of the detected peaks

The reference bursts can be affected in the same way as the DME signals (see Section 6.2). A reflected reference signal will arrive at the receiver with a delay as well as with an attenuation. If the signal strength is sufficient, it might give rise to a false reference.
When the reception of the direct and indirect pulses sufficiently overlap, the received pulse peak may shift in time. The peak detector of the receiver will detect the peak a bit later than without the interfering wind turbine. In the extreme case with a power ratio of the direct and indirect paths of 1, a half pulse width overlap of 1.75 µs will result in a maximum peak offset of 0.875 µs. The corresponding bearing offset is 0.005 degrees. This is much smaller than the overall TACAN bearing measurement accuracy of 1 degree and is therefore ignored further.

7.1.2 Phase shift of the measured AM-modulation

The AM-signal of the direct path is given by

$$D_{AM} = \mathrm{A} + \mathrm{B}\sin(30\pi t + \psi) + C\sin(270\pi t + 9\psi)$$

with ψ the bearing angle of the aircraft w.r.t. the reference and both the 15 Hz and 135 Hz modulations captured in the two sine terms. A, B, and C define the modulation depth of the AM-signal. In [8] the standard values are defined as A = 1, B = 0.21, and C = 0.21.

The indirect AM-signal of the reflected path is given by

$$R_{AM} = \sqrt{\frac{P_i}{P_d}}(\mathrm{A} + \mathrm{B}\sin(30\pi t + \psi + \phi) + C\sin(270\pi t + 9\psi + 9\phi)$$

with P_i/P_d the in Section 4.4 defined power ratio of the two paths and ϕ the angle from the aircraft to the wind turbine as seen by the TACAN.

The total received signal, is formed by a complex summation of the two paths. Two extreme situations can be identified, one with purely in-phase addition of the carrier, and one with purely antiphase additions of the carrier. Both will cause the phase of the direct-only signal to be shifted in opposite directions. The angular estimation errors in both extreme cases are shown in Figure 7.1 as function of the angle ϕ and the power ratio of the two paths. From this figure it can already be concluded that for common power ratios of smaller than -20 dB, the maximum error is about 0.6°.

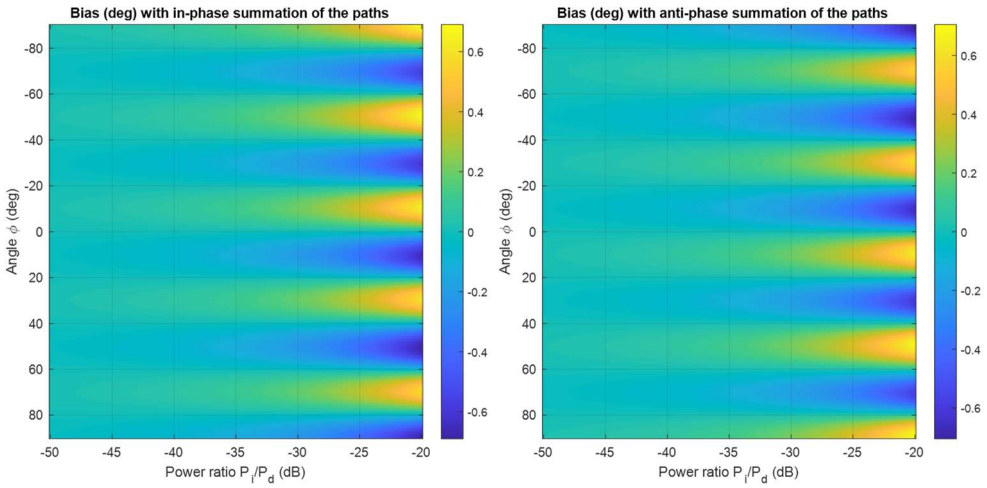

Figure 7.1 Maximum errors with purely in-phase (left hand figure) and purely antiphase (right hand figure) addition of the direct and indirect pulses. As can be seen when comparing the two figures, the error works in opposite directions. The errors are larger when the strength of the indirect path is relatively higher.

It is assumed that the maximum reflected power from the wind turbine blade can be present during the total 67 ms integration interval, since these so called blade flashes have a lifetime of about 100 to 150 ms. During the integration interval, the geometry of the turbine blade, the aircraft, and the TACAN antenna direction is not static. It is assumed that the carrier phase of the direct and indirect paths are random with respect to each other. Only if the relative change in path length would be within a fraction of the TACAN's wavelength (~0.30 m) over the complete integration time, this assumption is not valid. Considering the velocities of wind turbine blades and aircraft, the time interval in which the phase of the carrier signal could be assumed constant is in the order of 0.1 to 1 ms, which is 2 to 3 orders of magnitude shorter than the integration interval.

In reality due to the non-stationary geometry with motion of the aircraft and/or wind turbine blade, the complex summation has random phase from pulse to pulse. Therefore on average the measured phase error when integrating over at least a complete antenna revolution period of 67 ms will be zero. The phase shifts are the largest possible errors that theoretically could occur due to multipath for a stationary situation.

Please note that this error mechanism only occurs when the pulses of the two paths overlap. Otherwise the echo cancellation functionality will prevent the indirect pulses to be processed. Sufficient overlap is considered as at least half of the 3.5 µs pulse duration, with is equivalent to a maximum path length difference of 525 m. If the overlap is less, than the peak of the pulse will not be affected by the multipath.

7.2 Wind turbine RCS assumption

To determine the bearing accuracy, it is assumed that a blade is in a position providing maximum reflection towards the aircraft.

7.3 Propagation

For bearing determination, radio waves travel only from TACAN to aircraft.

7.4 Bearing error results for the wind turbines

For the wind turbines, the maximum (worst-case) absolute bearing errors that may occur as explained in 7.1.2, are analysed for the area that surrounds the TACAN and wind turbines as a function of the position of the aircraft. The results are valid for aircraft that fly at an altitude of 1,000 ft (305 m) with respect to the terrain height at the TACAN.

Figure 7.2 shows a generic example of the maximum possible bearing errors (in degrees), due to phase shift of the measured AM-modulation for a generic wind turbine located 10 km west of a TACAN for a grid of aircraft locations at an altitude of 1,000 ft (305 m) w.r.t. the terrain height at the TACAN.

The colour shows the absolute magnitude of the bearing error (in degrees) that could occur due to the addition of the directly and indirectly received pulses for a static situation. The error is a function of the angle between the wind turbine and the aircraft as seen from the TACAN and the relative strength of the direct and indirect path.

The error mechanism only applies when there is sufficient overlap of the pulses from the direct and indirect path. In this figure the area that surrounds the wind turbine corresponds to the area in which the indirect first pulse of a pulse pair overlaps with the direct first pulse. The ‘ring’-like area corresponds to the area in which the indirect first pulse of a pulse pair overlaps with the direct second pulse.

Please note, as already explained before that in a real, non-static situation the actual error due to this mechanism will cancel out. The errors as given below, are to be considered as a very worst case situation.

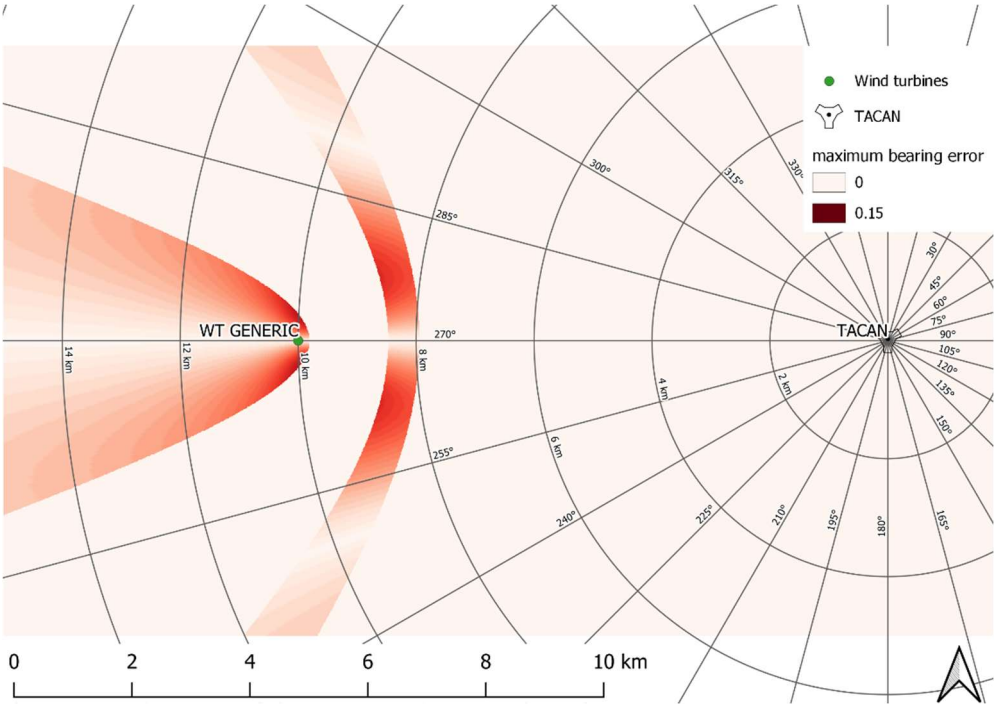

Figure 7.2. Example of maximum possible bearing errors (in degrees), due to phase shift of the measured AM-modulation for a generic wind turbine located 10 km west of a TACAN for an aircraft with altitude of 1,000 ft (305 m) w.r.t. the terrain height at the TACAN. The error mechanism only applies when there is sufficient overlap of the pulses from the direct and indirect path. In this figure the area that surrounds the wind turbine corresponds to the area in which the indirect first pulse of a pulse pair overlaps with the direct first pulse. The 'ring'-like area corresponds to the area in which the indirect first pulse of a pulse pair overlaps with the direct second pulse.

7.4.1 Bearing errors in degrees for WT1

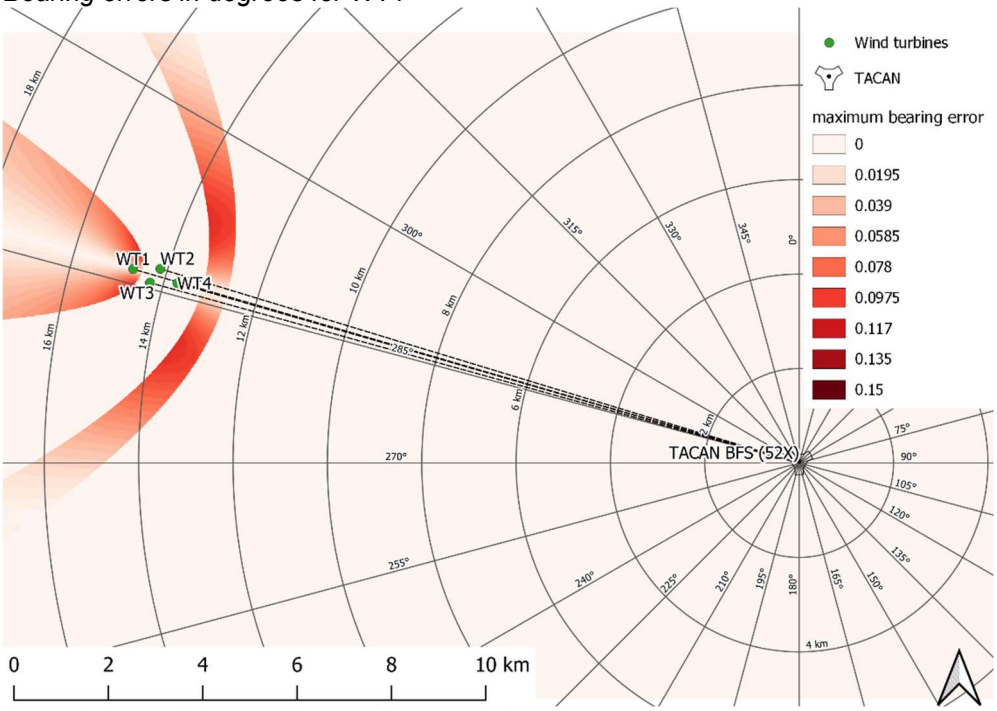

7.4.2 Bearing errors in degrees for WT2

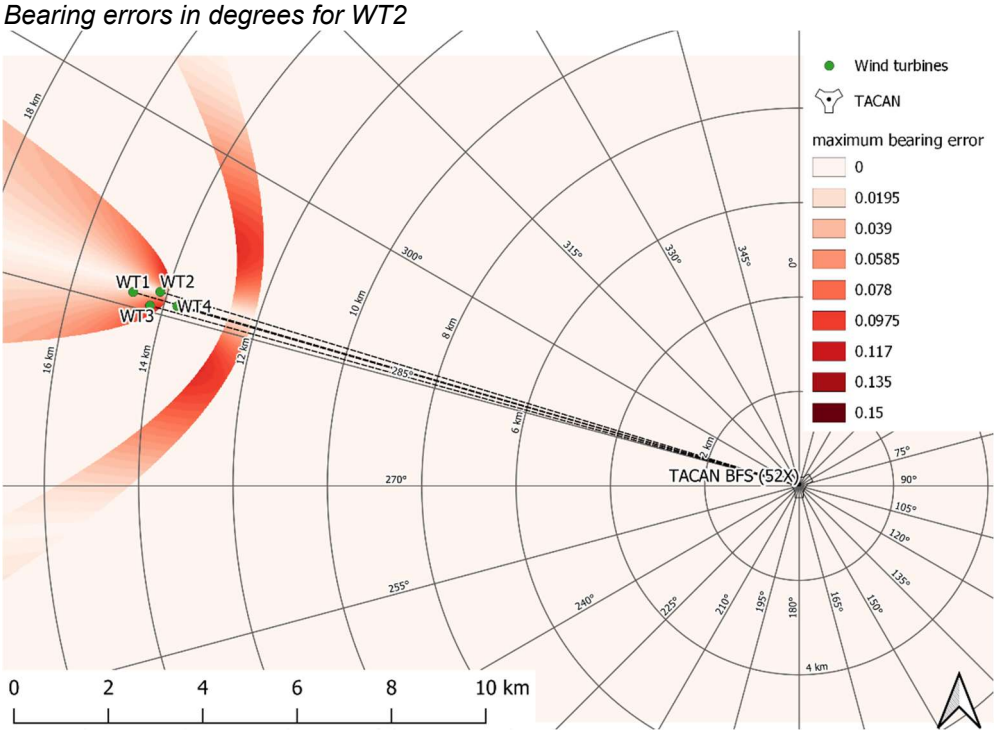

7.4.3 Bearing errors in degrees for WT3

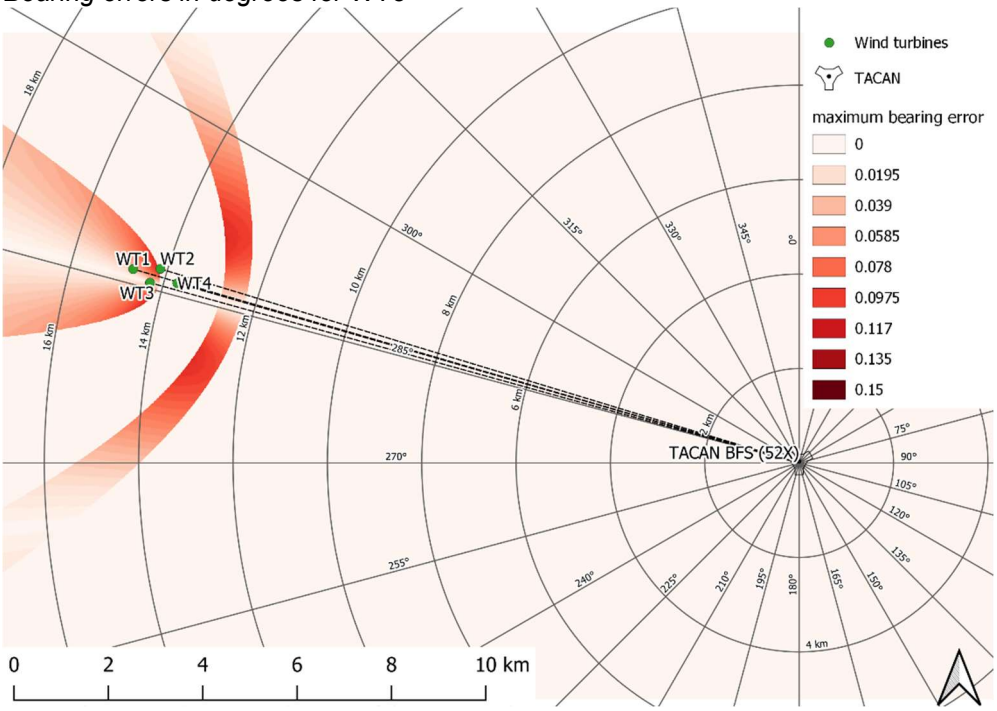

7.4.4 Bearing errors in degrees for WT4

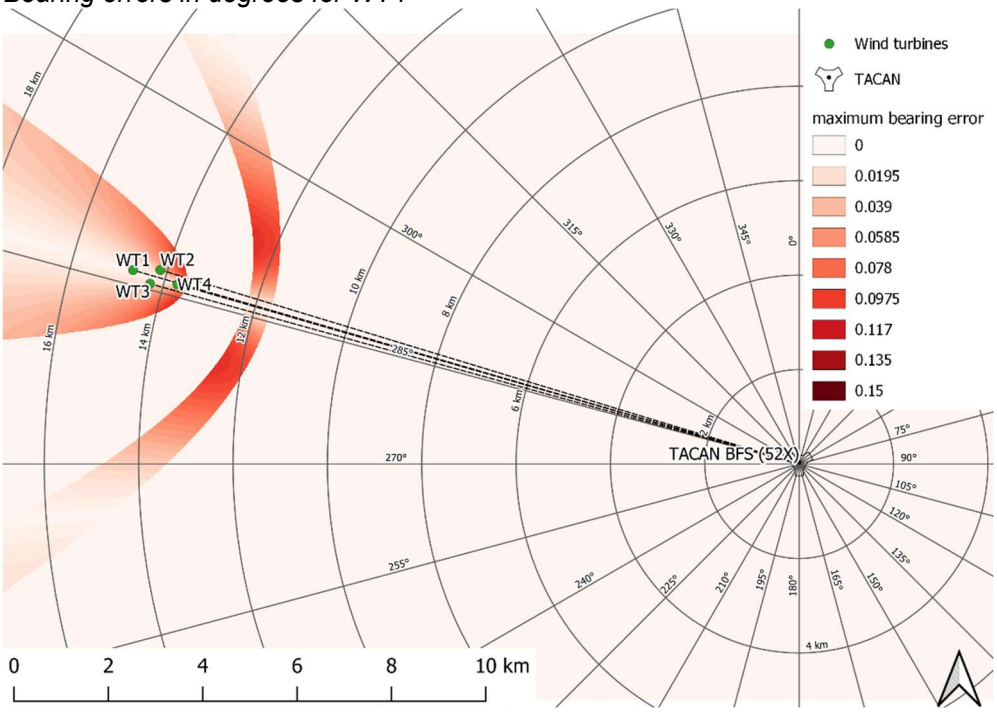

7.5 Consequences for TACAN bearing measurements

The analysis shows that the bearing accuracy of the 15 Hz and 135 Hz amplitude modulated signals is only marginally affected by the new wind turbines WT1, WT2, WT3, and WT4 with maximum errors of 0.1°.

This error is small in comparison to the TACAN overall bearing error, which is claimed to be ± 1°, [4].

Note that the analysis given here is based on the worst case scenario, a wind turbine blade in the most unfavourable position. This condition will only be present for a short time, due to both rotation of the wind turbine rotor and the movement of the aircraft. Under nominal conditions, the performance degradation of the TACAN system will be much less than described here.

8 Simple Engineering Assessment Beauvechain

8.1 Line of sight analysis

Using the information given in Chapter 2, we have carried out a line-of-sight analysis. In Figure 3.1 we show the terrain profile in the area containing the wind turbines and radars. The lines in the figure connect the radar to the planned wind turbines (New-WT1-New-WT4). By studying the terrain profile along this line for each wind turbine, we can determine whether the radar in Beauvechain will have line-of-sight to the windfarm.

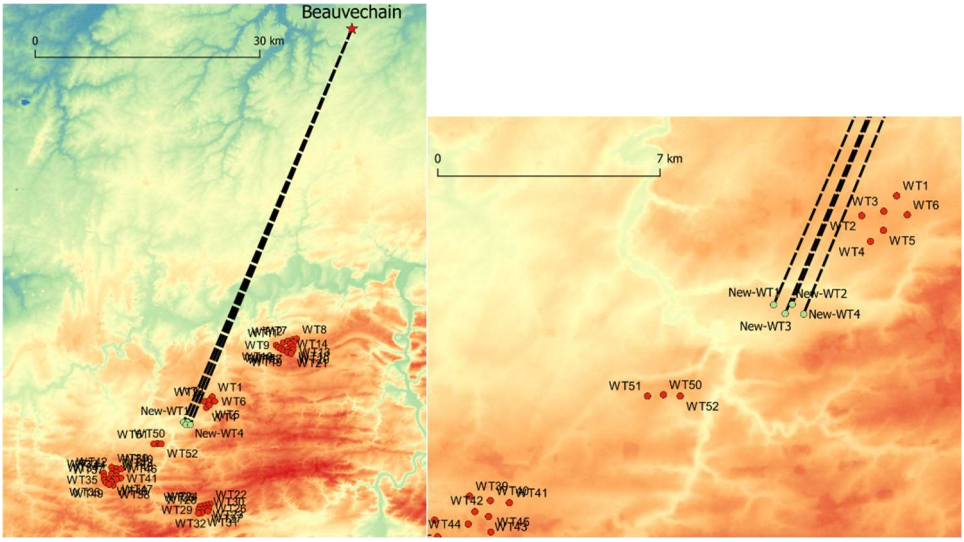

Figure 8.1 The altitude of the terrain between both the radar and the wind turbines taken from the SRTM database. The line-of-sight analysis is performed by studying the terrain profile on the line connecting the radar and each wind turbine.

So-called ‘standard propagation’ is assumed when determining the line-of-sight. This is modelled by multiplying the earth radius by a factor of 4/3 (the “k-factor”).

In the figures on the next pages the red ellipses show the first Fresnel zone from the radar antenna to the tip height of the wind turbine and the blue ellipses show the first Fresnel zones from the radar antenna to the hub height of the wind turbines. These ellipses are referred to as the ¼ λ Fresnel zone, where λ refers to the radar wavelength. Signals travelling between the terminals within the blue and red ellipses are at most 90° out of phase with respect to the signal that takes the shortest path. The black lines show the profile of the ground level between the radar and wind turbine as derived from the SRTM database[2].

8.1.1 Newly Planned Turbines

[2] For the line-of-sight analysis the data from the Shuttle Radar Topography Mission (SRTM1) is used. This database contains terrain altitude information with respect to the EGM96 geoid. The database was determined by NASA using high-resolution radar carried on the Space Shuttle. The SRTM data has a resolution of 1 arcseconds, which corresponds to a horizontal resolution of about ~20 m at 51 degrees latitude.

Figure 8.2 to Figure 8.5 show line-of-sight diagrams between the location of the radar system and the newly planned wind turbine locations. The horizontal range is range over ground in kilometres calculated using Vincenty's formulae. The turbines are located approximately 57 km from the PSR at Beauvechain.

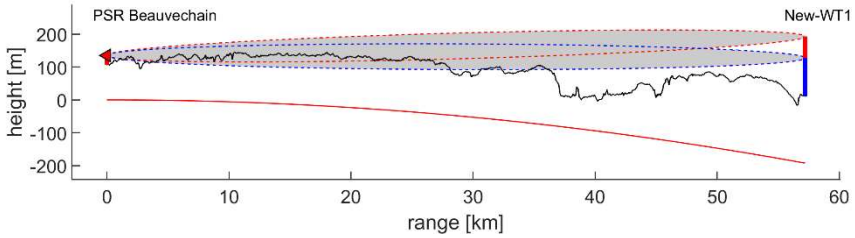

Figure 8.2 Line-of-sight between the PSR of Beauvechain and the newly planned wind turbine WT80. The distance from the radar to the wind turbine measures 57.2 km.

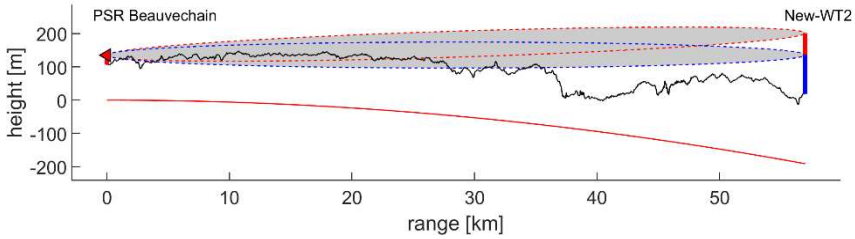

Figure 8.3 Line-of-sight between the PSR of Beauvechain and the newly planned wind turbine WT81. The distance from the radar to the wind turbine measures 57.0 km.

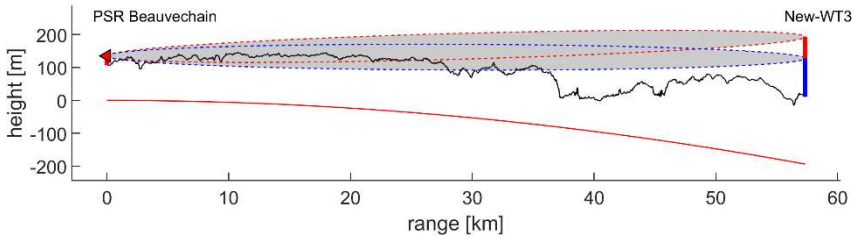

Figure 8.4 Line-of-sight between the PSR of Beauvechain and the newly planned wind turbine WT81. The distance from the radar to the wind turbine measures 57.3 km.

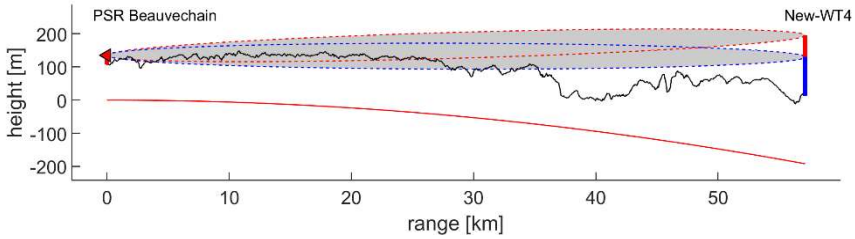

Figure 8.5 Line-of-sight between the PSR of Beauvechain and the newly planned wind turbine WT82. The distance from the radar to the wind turbine measures 57.1 km.

The Fresnel zones are not obstructed by the terrain profile, meaning that the radar antenna has line-of-sight to the planned wind turbines.

8.1.2 Existing, authorized and pending Turbines

Because the number of existing, authorized and pending turbines is large, not all line-of-sight figures for these turbines are presented. After investigation of the different line of sights to the PSR at Beauvechain it is determminde that two windfarm are close in range or in azimuth. These are windfarm (WT1-WT6) and windfarm Fontenelle (WT51-WT53). Figure 8.6 to Figure 8.8 show the corresponding line-of-sight plot for WT2 and WT3 and WT52 with are the closest in azimuth. these two turbines. As can be observed from the figures the Fresnel zones are not fully obstructed by the terrain profile, meaning that the radar antenna has line-of-sight to the wind turbines.

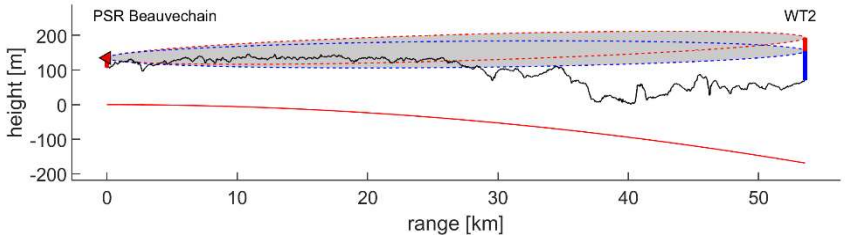

Figure 8.6 Line-of-sight between the PSR of Beauvechain and WT2. The distance from the radar to the wind turbine measures 53.6 km.

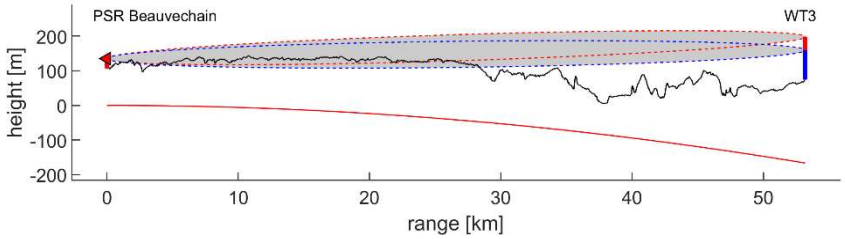

Figure 8.7 Line-of-sight between the PSR of Beauvechain and WT3. The distance from the radar to the wind turbine measures 53.6 km.

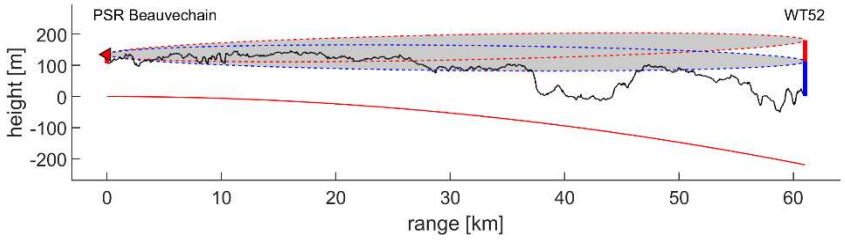

Figure 8.8 Line-of-sight between the PSR of Beauvechain and WT52. The distance from the radar to the wind turbine measures 61.0 km.

8.2 Regions of potential Impact

8.2.1 Introduction

In Chapter 3 we have determined that the radar has line-of-sight to all wind turbines. When this is the case the wind turbines can affect the radar in a number of ways. The EUROCONTROL guidelines [1] prescribe that in the case of a simple engineering assessment, the size of the following two regions must be determined:

1. The shadow region behind the wind turbine, caused by the attenuation due to the wind turbine being an obstacle for the electromagnetic field.
2. The volume located above and around the wind turbine in which the radar detection threshold, generally implemented with CFAR (Constant False Alarm Rate) logic, is affected.

Both regions are shown in Figure 8.9 below. This image was taken from [1], Section 4.3.1. In the next sections the size of the two regions are determined.

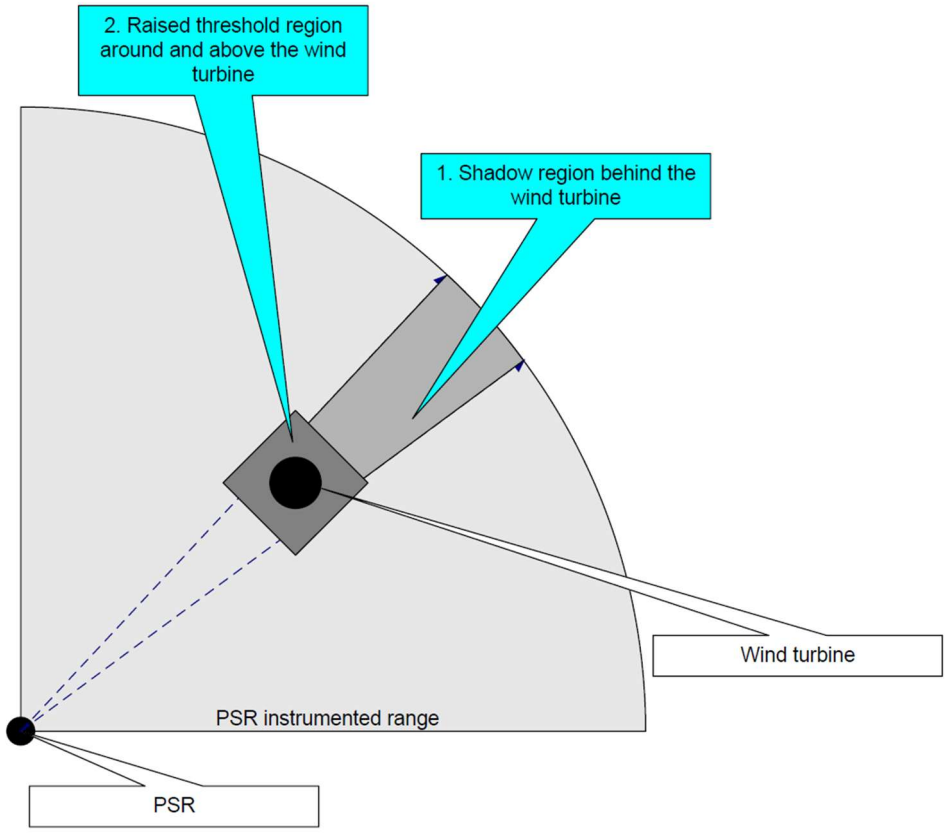

Figure 8.9 Schematic representation of the shadow region behind a wind turbine (1) and the raised threshold region around and above a wind turbine. Image taken from [1].

8.2.2 *Region 1: Shadow region*

In this section we determine the size of the shadow regions behind the wind turbine. In Figure 8.10 the shape of the region is shown. The shadow region extends all the way to the instrumented range of the radar. The length of the shadow region is therefore equal to the instrumented range minus the distance from the radar to the wind turbine. The width of the shadow region is given by $2\sqrt{(\lambda D)}$, where λ is the radar wavelength and D the distance from the wind turbine. See also Annex A-3 in the EUROCONTROL guidelines [1]. The width is at its maximum at the instrumented range from the radar.

Finally, the height of the shadow region can be calculated according to Equation 1 in Annex A-2 in [1]. Note that this calculation takes the curvature of the earth into account by assuming a spherical earth with radius kR_e, where R_e is the earth radius and k is the standard propagation k-factor equal to 4/3. The calculated height is relative to the EGM96 geoid, which is approximately equal to mean sea level and is accurate within several meters. The height of the shadow region is equal to the tip height at the location of the wind turbine and increases (not taking the ground level into account) to its maximum value at instrumented range from the radar.

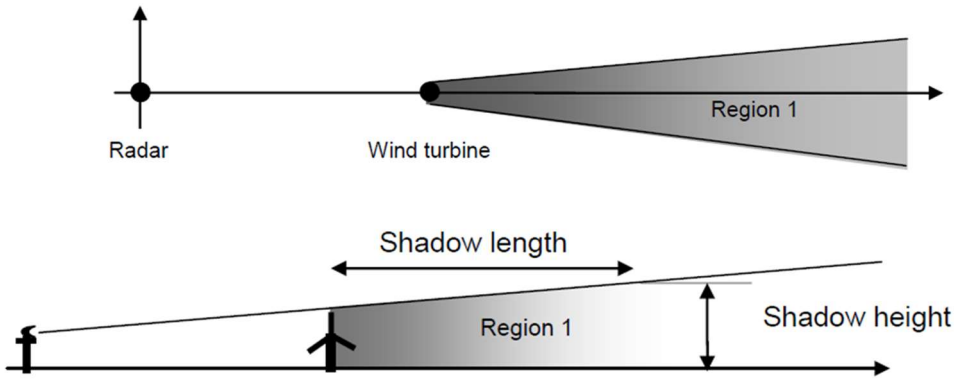

Figure 8.10 Shape of the shadow region. Image taken from Annex A-1 in [1].

In contradiction to an optical shadow, a wind turbine in the line of sight path will affect visibility, but not in all cases causes the target to be invisible. This principle is illustrated in Figure 8.11. Radio waves diffract around an obstacle, limiting the shadow zone directly behind an obstacle. Due to the fact that energy is reflected back from the wind turbine the presence of a wind turbine will cause a loss in maximum detection range.

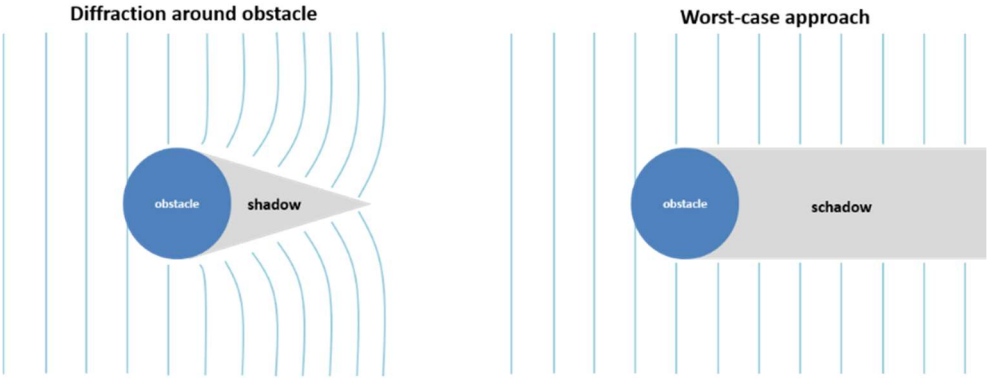

Figure 8.11 Graphical illustration of diffraction effects.

8.2.3 Shadow Locations PSR Beauvechain

The shadows of all turbines for PSR Beauvechain (existing, authorized, pending and planned) are presented in Figure 8.13. The geographic locations of the shadows of the planned turbines for PSR Beauvechain are shown in Figure 8.12. The shadows of the existing, authorized and pending turbines are indicated with black, the shadows of the planned turbines are indicated with a red colour. It can be observed that the shadows of the planned turbines do not overlap with the shadows of the existing turbines.

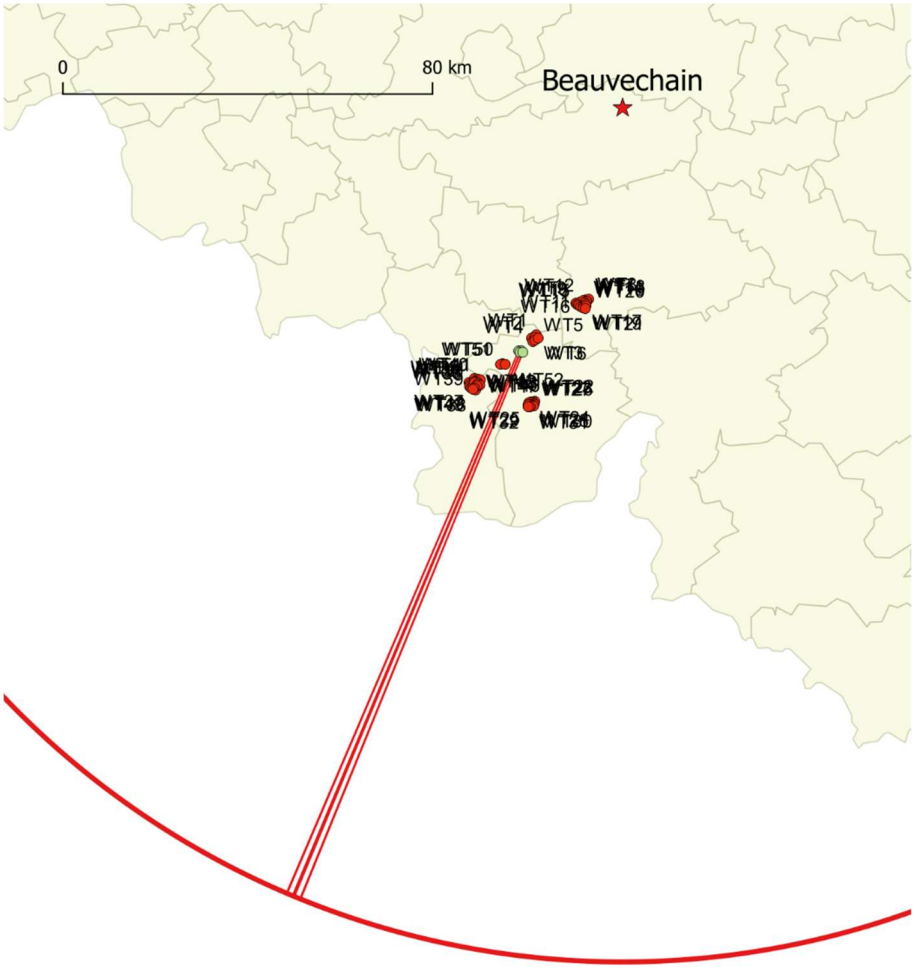

Figure 8.12 The geographic locations of the shadow regions of only the new turbines as seen from the PSR in Beauvechain. The shadow regions (small red regions) extend from the wind turbine to the instrumented range (100 NM or 185 km) of the radar (indicated with a red circle).

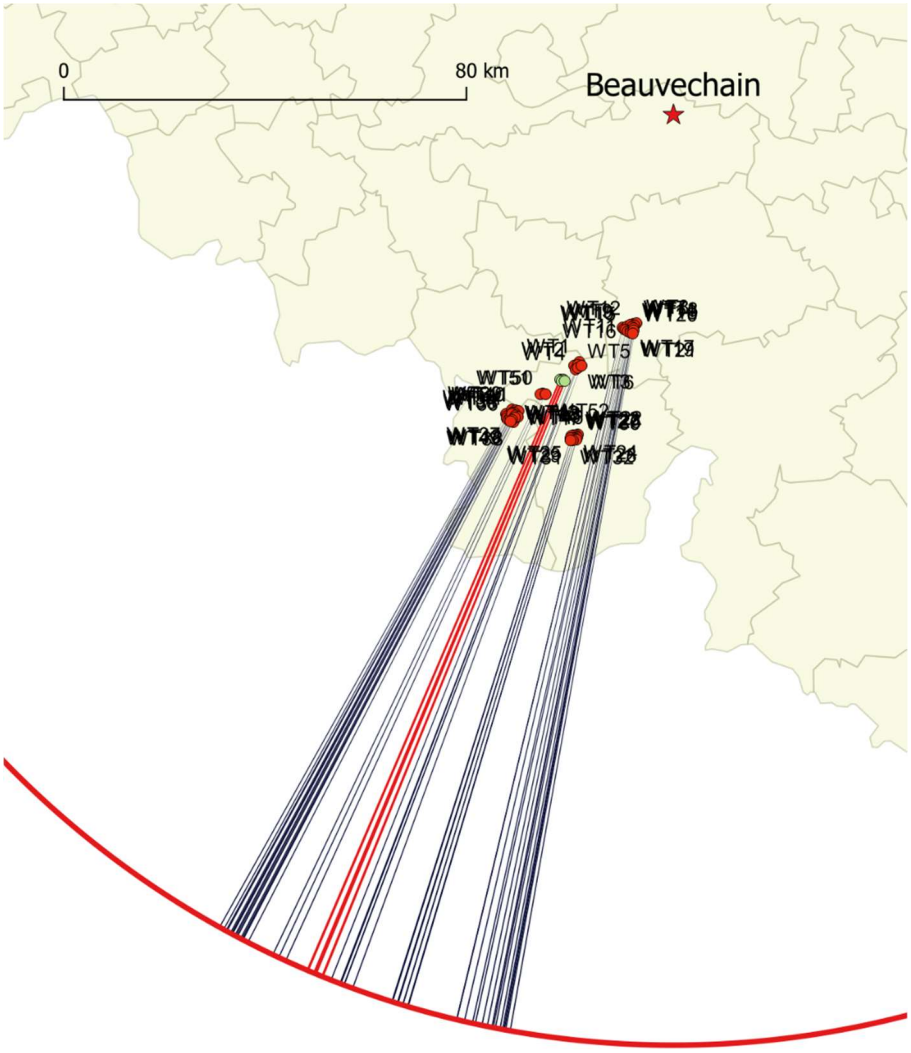

Figure 8.13 The geographic locations of the shadow regions of all turbines as seen from the PSR in Beauvechain. The shadow regions of the planned (small red regions) and existing, authorized and pending turbines (small black regions) extend from the wind turbine to the instrumented range (100 NM or 185 km) of the radar (indicated with a red circle).

8.2.4 Shadow Dimensions PSR Beauvechain

No shadows of existing, authorised or pending wind turbines overlap with the shadows of the new wind turbines. As such, no length, maximum width and maximum height of the shadow regions for the existing wind turbines are. The maximum shadow width and height for the newly planned turbines are provided in Table 8.1.

Table 8.1 Dimensions of the shadow regions of the four new wind turbines.

Nr.	ID	Tip Height [m]	Shadow PSR Beauvechain		
			Length [km]	Max. height w.r.t. sea level [km]	Max. Width [m]
53	New-WT1	182.5	127.75	2.336	233.909
54	New-WT2	182.5	127.98	2.365	234.120
55	New-WT3	182.5	127.62	2.336	233.790
56	New-WT4	182.5	127.83	2.345	233.982

8.2.5 Region 2: Raised threshold regions

The second region of potential impact is the so-called raised threshold region. In this region the possibly large reflection of the wind turbine raises the detector threshold of the radar, lowering the probability of detection of a target.
The size of the region in range is dependent on the exact implementation of the CFAR detection logic in the radar. In general a radar threshold is determined using a number of range cells around the Cell Under Test (CUT).
In the case of PSR Beauvechain (see Table 2.6) the number of range cells around the cell under test has been specified to be 24 In addition the 12 closest range cells, the so-called guard cells, are neglected. Given the size of a range cell of 21.9 m, we calculate that a wind turbine can potentially influence the radar threshold from approximately 788 m in front until 788 m behind the wind turbine. The size in azimuth is dependent on the horizontal beam width of the radar. Given the beam width in Table 2.6, at a range of 25 km the size in azimuth is approximately 655 m.

The region in which the wind turbine influences the threshold has been calculated for 2 combinations of wind turbines and radars:

1. The existing, authorized and pending turbines that are closest in range from the planned wind turbines.
2. All mentioned in 1. and the newly planned wind turbines.

The results are presented in Figure 8.14 and Figure 8.15. There is no overlap between the regions of the existing and newly planned wind turbines. The affected area due to the new wind turbines is 7.32 km^2 for PSR Beauvechain.

Figure 8.14 The raised threshold regions (indicated with the orange regions) for the existing and authorized turbines closest to the newly planned turbines for PSR Beauvechain.

Figure 8.15 The raised threshold regions for all existing, authorized and pending turbines (indicated with the orange regions) and new turbines (indicated with the green regions) for PSR Beauvechain.

The pictures above should be interpreted with care, for two reasons. Firstly, the scattering properties of the moving and the non-moving parts of the wind turbines

are not being considered. With respect to the non-moving parts: since wind turbine masts are often shaped like truncated cones, wind turbine mast backscatter is not being sensed by the radar, as illustrated in Figure 8.16, given the distance to the wind farm.

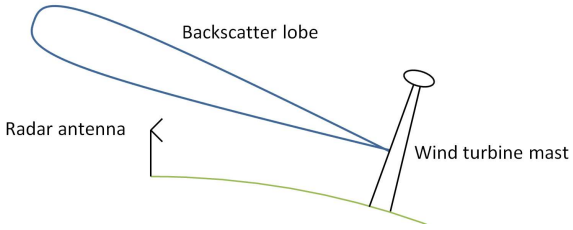

Figure 8.16 Due to the earth curvature as well as the tapering of the wind turbine mast diameter, wind turbine mast backscatter, which is confined in the backscatter lobe, may not be received by the radar. This physical phenomenon is neglected in Figure 8.14 and Figure 8.15.

8.3 False target reports and processing overload

Modern surveillance radars are equipped with multiple mechanism to obtain detections of flying targets only. To suppress reflections at non-moving objects, adaptive cluttermaps are maintained, potentially within each Doppler filter. Non-moving structures, such as the wind turbine mast and the nacelle will therefore not give rise to false (non-target) plots. A flying target will be detected if its response (echo) also passes the so-called CFAR (constant false alarm rate) circuitry. Radar manufacturers have responded to the detection of wind turbine blade flashes, by adapting the logic of the CFAR process. Rather than the CAGO (cell averaging greatest of) logic, ordered statistics (OS) logic is nowadays often applied, since this processing is better capable to detect aircraft when a wind turbine blade flash occurs. Note that the Belgium Airforce has indicated that the Beauvechain radaris equipped with CAGO CFAR circuitry (rather than OS or like circuitry).

The Beauvechain radar has been equipped with a modern Next Generation Signal Processor (NGSP) receiver from Intersoft-Electronics. Therefore the radar benefits from the Vertical Clutter Canceller or VCC technology. With this technology the radar is capable of adapting the elevation antenna pattern on receive, range dependent. Thus, wind turbine backscatter can be ‘nulled’, which improves the detection capability of the radar above wind turbines.

The maximum rotation speed of a wind turbine is assumed to be 30 rpm. Each rotation produces six Doppler flashes, three negative and three positive, when one of the three blades is pointing up- or downwards. This results in a worst case flash frequency of 3 Hz per wind turbine. Given this blade flash frequency of 3 Hz, three additional wind turbines, the azimuth beamwidth and the antenna rotation rate, 0.25 blade flashes per scan are expected from the entire windfarm for the PSR at Beauvechain. This is a worst case assumption, which neglects the several anti-wind turbine features of these radars described above, is that these flashes will result in PSR-only plots. Since modern surveillance radars are capable to process several hundred plots per second, the extra plots are considered as being insignificant. Processing overload is therefore not expected.

9 Conclusions

9.1 Engineering Assessment TACAN Florennes

The main conclusion of this analysis are:

1. There is no negative influence of the wind turbine on the TACAN DME accuracy found based on a worst-case situation. Even in exceptional circumstances, and only at low altitudes in specific regions, the TACAN will not be erroneously triggered to transmit a second reply on a single DME interrogation. Airborne DME-equipment is deemed to be sufficiently protected to these rare situations by means of 'echo cancellation'.

2. The TACAN bearing error augments to maximally 0.1° in a worst-case situation. This is small with respect to the overall claimed bearing error of ± 1°. This error only applies to static, theoretical situations. In reality the error due to this mechanism will be much smaller or even absent.

The above mentioned conclusions assume that the TACAN system works with properly implemented dead time and that aircraft navigation equipment have proper 'echo cancellation' functionality.

Please note that the conclusions are based on a worst case scenario. Under nominal conditions, the performance degradation of the TACAN system will be much less than stated above.

9.2 Simple Engineering Assessment Beauvechain

In accordance with EUROCONTROL's description of a simple engineering assessment for primary radar systems, three subjects have been analysed: line-of-sight, the volumes of the regions that are impacted, and the occurrence of false target reports.

It is concluded that the new wind turbines are not significantly obstructed by altitude level of the terrain between the radar installation and the wind turbine. The size of the volume in which radar degradation occurs has been specified in Section 8.2.5 of the document. The newly planned wind turbines will create a volume where the PSR at Beauvechain can potentially be desensitised of 7.32 km^2 at a distance of approximately 57 km from the radar.

Due to the cluttermap processing, it is not expected that static structures of the wind turbines will raise alarms. The probability that an alarm will be induced as a consequence of a wind turbine blade flash has been elaborated in Section 8.3. The increase of the plot rate due to this phenomenon is expected to be negligible.

9.3 Changes to the wind turbine configuration

As stated in Section 2.1 the absence of the three wind turbines at Fontenelle and the two additional wind turbines at Walcourt Florennes Gerpinnes do not have an influence on the outcomes of both studies mentioned above.

10 List of abbreviations

AFB	Air Force Base
AGL	Above Ground Level
AMSL	Above Mean Sea Level
ARB	Auxiliary Reference Burst
ASR	Airfield Surveillance Radar
CAGO	Call Averaging Greatest Of
CFAR	Constant False Alarm Rate
CUT	Cell Under Test
DME	Distance Measuring Equipment
EGM96	Earth Gravitational Model 1996
MRB	Main Reference Burst
NASA	National Aeronautics and Space Administration
NGSP	Next Generation Signal Processor
OS	Ordered Statistics
PSR	Primary Surveillance
RCS	Radar Cross Section
RPM	Revolutions Per Minute
SSR	Secondary Surveillance Radar
SRTM	Shuttle Radar Topography Mission
TACAN	TACtical Air Navigation system
TNO	Netherlands Organisation for Applied Scientific Research
VCC	Vertical Clutter Cancellation
WGS84	World Geodetic System 1984
WT	Wind Turbine

11 References

[1] eAIP Belgium & Luxembourg, Part 3 Aerodromes, effective date 31 DEC 2020
eAIP Belgium and Luxembourg (skeyes.be)

[2] TACAN explanation on “Aviation” (Aviation stack exchange, a website with Q & a for pilots. Website:
https://aviation.stackexchange.com/questions/27689/how-does-tacan-work

[3] TACAN explanation on radio navigational aids, a website on radar and radio navigation. Website:
http://www.radarpages.co.uk/mob/navaids/tacan/tacan1.htm

[4] TACAN explanation on Wikipedia:
https://en.wikipedia.org/wiki/Tactical_air_navigation_system

[5] Electronics technician Volume 5: Navigation Systems:
Chapter 2: Tactical Air Navigation (TACAN)
http://electronicstechnician.tpub.com/14090/css/Chapter-2-Tactical-Air-Navigation-31.htm

[6] Testing of DME/TACAN Ground Stations, Rohde & Schwarz,
https://cdn.rohde-schwarz.com/pws/dl_downloads/dl_application/application_notes/1ef91/1EF91[7_2e_DME_TACAN_Gstations.pdf]

[8] MIL-STD-291, STANDARD TACTICAL AIR NAVIGATION (TACAN) SIGNAL, 10 February 1998.

[9] EUROCONTROL guidelines on How to Assess the Potential Impact of Wind Turbines on Surveillance Sensors, Edition 1.2, September 2014, Ref. nr EUROCONTROL-GUID-0130.

[10] TA10M Radar file ASR Beauvechain v.D.1.0 received from the Belgium Ministry of Defence.

[11] E-mail “Re: Request for information (new?)” regarding the update the TA10M recently has received Domien De Ruyck of MRCI-DEOMATIC3D dated 15th February 2018.